

Oral Communications

15.^{as} Jornadas de Formación del Centro de Investigación Biomédica en Red de Enfermedades Respiratorias (CIBERES)

Madrid, 24 y 25 de noviembre de 2022

17. DEVELOPMENT AND VALIDATION OF MACHINE AND DEEP LEARNING ALGORITHMS FOR DETECTING FLOW DYSSYNCHRONY IN MECHANICALLY VENTILATED CRITICALLY ILL PATIENTS DURING ASSISTED-VOLUME CONTROL VENTILATION

Verónica Santos-Pulpón^{1,2}, Leonardo Sarlabous^{1,2}, Andrés Oswaldo Pérez-Trenard¹, Rudys Magrans³, Josefina López-Aguilar^{1,2}, Sol Fernández-Gonzalo^{1,4,5}, Guillem Navarra^{1,2}, Gemma Gomà^{1,2}, Oriol Roca^{1,2,6}, Guillermo Muñiz-Albaiceta^{2,7}, Gastón Murias⁸, Rafael Fernández^{2,9}, Candelaria de Haró^{1,2}, Lluís Blanch^{1,2}

¹Critical Care Center Hospital Universitari Parc Taulí Institut d'Investigació i Innovació Parc Taulí I3PT, Sabadell, Spain. ²Centro de Investigación Biomédica en Red en Enfermedades Respiratorias (CIBERES), Madrid, Spain. ³Bettercare, Sabadell, Spain. ⁴Centro de Investigación Biomédica En Red en Salud Mental (CIBERSAM), Madrid, Spain. ⁵Department of Clinical and Health Psychology Universitat Autònoma de Barcelona, Barcelona, Spain. ⁶Departament de Medicina UAB, Barcelona, Spain. ⁷Unidad de Cuidados Intensivos Hospital Universitario Central de Asturias Departamento de Biología Funcional Universidad de Oviedo, Oviedo, Spain. ⁸Servicio de Terapia Intensiva del Hospital Británico de Buenos Aires, Buenos Aires, Argentina. ⁹Intensive Care Unit Fundació Althaia Universitat Internacional de Catalunya, Manresa, Spain.

Introduction: An excessive respiratory drive may lead to vigorous inspiratory efforts which can result in detrimental lung distending pressures in critically ill patients undergoing invasive mechanical ventilation. Early detection of these events is necessary to avoid potential adverse effects.

Objectives: To develop a supervised artificial intelligence algorithm that allows to classify respiratory pressure cycles triggered by patients, on assisted-volume control ventilation, into one of the expert-classified flow dyssynchrony patterns.

Methods: Twenty critically ill adults undergoing mechanical ventilation > 24 hours, with available registered ventilatory waveforms were included. Three patterns of flow dyssynchrony were defined by experts as normal, moderate and severe. Expert visual assessment was considered the gold standard. Three models were used for the time series classification task: 1) a combination of dynamic time warping + nearest neighbours with K = 1 (DTW + 1-NN), 2) a recurrent neural

network (RNN) and 3) a one-dimensional convolutional neural network (1D-CNN).

Results: A total of 5,907 breaths from 20 patients were analysed. The incidence of patterns was not balanced: 2,666 being classified normal cycles, 1,306 moderate and 1,935 severe. The accuracy for the DTW + 1-NN machine learning model was 87.6% for validation, while for the RNN and 1D-CNN deep learning models it was 90.3% and 90.2% for training, and 89.6% and 89.4% for validation, respectively. The best accuracy was obtained for LSTM-RNN with accuracy = 0.894%, recall = 0.896% and F1-score = 0.894%.

Conclusions: Our study suggests that the recurrent neural network is able to classify expert-defined flow dyssynchrony patterns with high precision, accuracy and recall. This model can potentially provide a good tool to facilitate quantification of the incidence of flow dyssynchrony during the entire period of mechanical ventilation.

Funding: This work has been funded by: RTC-2017-6193-1 (AEI/FEDER EU). 202118-30 Fundació La Marató de TV3. Verónica Santos-Pulpón was supported by the CIBER of Respiratory Diseases. Leonardo Sarlabous was supported by the PERIS programme of the Department of Health of the Generalitat de Catalunya.

14. EFFECTS OF INTUBATION TIMING IN PATIENTS WITH COVID-19 THROUGHOUT THE FOUR WAVES OF THE PANDEMIC: A MATCHED ANALYSIS

Enric Barbeta¹, Jordi Riera del Brío², Adrián Tormos³, Ricard Mellado-Artigas¹, Adrián Ceccato⁴, Anna Motos¹, Laia Fernandez¹, Darío García-Gasulla¹, Carlos Ferrando¹, Ferran Barbé⁵, Antoni Torres¹

¹Hospital Clínic de Barcelona, Barcelona, Spain. ²Hospital Vall d'Hebron, Barcelona, Spain. ³Barcelona Supercomputing center, Barcelona, Spain. ⁴Hospital Parc Taulí, Barcelona, Spain. ⁵Hospital Arnau de Vilanova, Barcelona, Spain.

Introduction: It remains unknown whether delay in intubation worsens clinical outcomes in acute respiratory failure due to COVID-19.

Objectives: To investigate the association between intubation timing and hospital mortality in critically ill patients with COVID-19-associated respiratory failure. We also analysed both the impact of such

timing throughout the first four pandemic waves and the influence of prior non-invasive respiratory support on outcomes.

Methods: This is a secondary analysis of a multicentre, observational and prospective cohort study that included all consecutive patients undergoing invasive mechanical ventilation due to COVID-19 from across 58 Spanish intensive care units (ICU) participating in the CIBERESUCICOVID project. The study period was between 29 February 2020 and 31 August 2021. Early intubation was defined as that occurring within the first 24 hours of intensive care unit (ICU) admission. Propensity score (PS) matching was used to achieve balance across baseline variables between the early intubation cohort and those patients who were intubated after the first 24 hours of ICU admission. We performed sensitivity analyses to consider a different timepoint (48 hours from ICU admission) for early and delayed intubation.

Results: Of the 2,725 patients who received invasive mechanical ventilation, a total of 614 matched patients were included in the analysis (307 for each group). After PS matching, patients with delayed intubation presented higher hospital mortality (27.3 vs. 37.1%, $p = 0.01$), ICU mortality (25.7 vs. 36.1%, $p = 0.007$) and 90-day mortality (30.9 vs. 40.2%, $p = 0.02$) when compared to the early intubation group. Very similar findings were observed when we used a 48-hour timepoint for early or delayed intubation. The use of early intubation decreased after the first wave of the pandemic (72%, 49%, 46% and 45% in the first, second, third and fourth wave, respectively; $p < 0.001$). In both the main and sensitivity analyses, hospital mortality was lower in patients receiving high-flow nasal cannula ($n = 294$) who were intubated earlier. The subgroup of patients undergoing NIV ($n = 214$) before intubation showed higher mortality when delayed intubation was set as that occurring after 48 hours from ICU admission, but not when after 24 hours.

Conclusions: In patients with COVID-19 requiring invasive mechanical ventilation, delayed intubation was associated with a higher risk of hospital mortality. The use of early intubation significantly decreased throughout the course of the pandemic. Benefits of such an approach occurred more notably in patients who had received high-flow nasal cannula.

Funding: Financial support was provided by the Instituto de Salud Carlos III de Madrid (COV20/00110, ISCIII), Fondo Europeo de Desarrollo Regional (FEDER), "Una manera de hacer Europa", and the Centro de Investigación Biomedica En Red - Enfermedades Respiratorias (CIBERES).

35. THE IMPORTANCE OF DRIVING PRESSURE AND ADJUNCTIVE THERAPIES IN PULMONARY SEQUELAE OF COVID-19 PATIENTS RECEIVING INVASIVE MECHANICAL VENTILATION. THE CIBERESICU SCORE

Jessica González¹, Ivan David Benítez¹, David de Gonzalo-Calvo¹, Anna Motos², Antoni Torres², Ferran Barbé³

¹Translational Research in Respiratory Medicine, University Hospital Arnau de Vilanova and Santa Maria, IRBLleida, Lleida, Spain. CIBER of Respiratory Diseases (CIBERES), Institute of Health Carlos III, Madrid, Lleida, Spain. ²Department of Pneumology, Hospital Clinic of Barcelona; August Pi i Sunyer Biomedical Research Institute-IDIBAPS, University of Barcelona, Barcelona, Spain CIBER of Respiratory Diseases (CIBERES), Institute of Health Carlos III, Madrid, Spain., Barcelona, Spain.

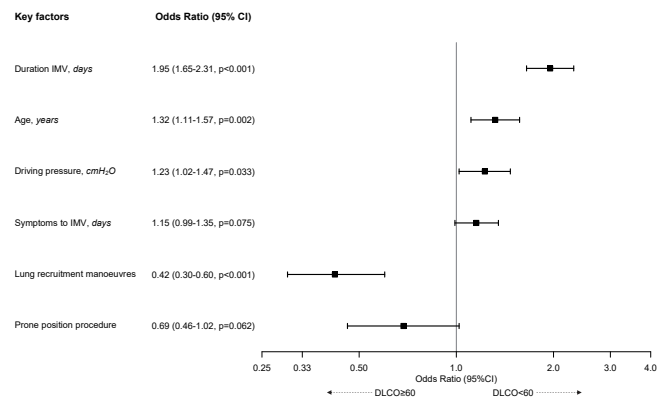
³Translational Research in Respiratory Medicine, University Hospital Arnau de Vilanova and Santa Maria, IRBLleida, Lleida, Spain. CIBER of Respiratory Diseases (CIBERES), Institute of Health Carlos III, Madrid, Lleida, Spain.

Introduction: Predictive factors of lung diffusing capacity (DLCO) impairment after invasive mechanical ventilation (IMV) due to COVID-19 are unknown.

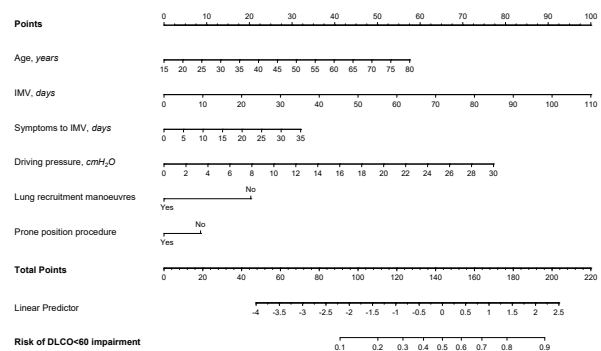
Objectives: Our objective was to identify the predictors of an impairment of DLCO (< 60%) in patients who needed IMV due to COVID-19.

Methods: This is a multicentre, prospective observational study in 51 Spanish intensive care units (ICUs). A total of 861 PCR-confirmed coronavirus disease 2019 (COVID-19) patients receiving IMV were included. At hospital admission, we collected sociodemographic, anthropometric, comorbidity and lifestyle data. Moreover, in-hospital clinical and biological parameters, ventilatory parameters and adjunctive therapies at three IMV time points (day one, three and the last day), and lung function and computed tomography findings at follow-up were assessed.

Results: The median (p25-p75) time from discharge to follow-up was 3.5 (2.7-4.7) months. The median age was 61 (53-67) years, and 26.9% were women. The mean (SD) percentage of predicted DLCO at follow-up was 70.3% (18%), with 27.5% of patients with a DLCO < 60%. Predictive factors for DLCO < 60% were (1) length of IMV (OR: 1.95 (1.65-2.31, $p < 0.001$)), (2) age (OR: 1.32 (1.11-1.58, $p = 0.002$)), (3) driving pressure (OR: 1.23 (1.02-1.47, $p = 0.033$)), (4) time from symptoms to intubation (OR: 1.15 (0.99-1.35, $p = 0.059$)), (5) prone positioning (OR: 0.69 (0.46-1.02, $p = 0.062$)), and (6) lung recruitment manoeuvres (LRMs) (OR: 0.42 (0.30-0.60, $p < 0.001$)) (Figure, panel A). A clinical scoring tool, named the CIBERESICU SCORE, was developed considering these predictors (Figure, panel B).



PANEL A



PANEL B

Panel A: Factors associated with DLCO impairment included in final multivariate model; Panel B: Characteristics in the nomogram to predict probability of DLCO impairment after hospital discharge in critical COVID-19 patients.

Baseline sociodemographic and clinical characteristics (at hospital and ICU admission) according DLCO impairment at follow-up visit

	DLCO ≥ 60 (n = 624)	DLCO < 60 (n = 237)	p-value	n
	Median [p25;p75] or n (%)	Median [p25;p75] or n (%)		
Sociodemographic data				
Sex, female	164 (26.3%)	68 (28.7%)	0.531	861
Age, years	60.0 [52.0;67.0]	63.0 [58.0;68.0]	< 0.001	861
Body mass index, kg/m ²	29.6 [26.5;33.2]	28.3 [26.4;31.5]	0.007	820
Smoking history			0.133	832
Former	209 (34.9%)	97 (41.6%)		
Non smoker	362 (60.4%)	123 (52.8%)		
Current	28 (4.67%)	13 (5.58%)		
Alcohol consumption			0.171	820
Former	6 (1.02%)	6 (2.62%)		
Non consumer	559 (94.6%)	216 (94.3%)		
Current	26 (4.40%)	7 (3.06%)		
Drug use			0.999	816
Former	5 (0.85%)	2 (0.87%)		
Non consumer	579 (98.8%)	228 (99.1%)		
Current	2 (0.34%)	0 (0.00%)		
Comorbidities				
Obesity	268 (42.9%)	72 (30.4%)	0.001	861
Hypertension	273 (43.8%)	126 (53.2%)	0.016	861
Diabetes mellitus (Type I/II)	115 (18.4%)	43 (18.1%)	0.999	861
Chronic heart disease	46 (7.37%)	35 (14.8%)	0.001	861
Chronic renal disease	18 (2.88%)	15 (6.33%)	0.031	861
Chronic moderate liver disease	3 (0.48%)	4 (1.69%)	0.095	861
Chronic mild liver disease	18 (2.88%)	3 (1.27%)	0.259	861
Chronic neurological disease	21 (3.37%)	16 (6.75%)	0.046	861
Chronic pulmonar disease	40 (6.41%)	26 (11.0%)	0.035	861
COPD	18 (2.88%)	16 (6.75%)	0.016	861
Bronchiectasis	0 (0.00%)	2 (0.84%)	0.076	861
Other	22 (3.53%)	8 (3.38%)	0.999	861
Asthma	34 (5.45%)	20 (8.44%)	0.145	861
Dementia	0 (0.00%)	1 (0.42%)	0.275	861
Rheumatic disease	32 (5.13%)	16 (6.75%)	0.447	861
Gastrointestinal/pancreatic disorders	47 (7.53%)	22 (9.32%)	0.471	860
Endocrine disorders	47 (7.53%)	12 (5.06%)	0.259	861
Metabolic disorders	164 (26.3%)	60 (25.3%)	0.840	861
Genitourinary disorders	27 (4.33%)	18 (7.59%)	0.080	861
Hematology disorders	20 (3.21%)	11 (4.64%)	0.420	861
Malignant neoplasm	12 (1.92%)	10 (4.22%)	0.096	861
HIV	2 (0.32%)	1 (0.42%)	0.999	861
Immunological disorders	5 (0.80%)	5 (2.11%)	0.149	861
Solid organ transplantation	1 (0.16%)	5 (2.11%)	0.007	861
Hospital admission in the last 30 days	7 (1.12%)	7 (2.95%)	0.071	861
Other risk factors	167 (26.8%)	67 (28.3%)	0.730	860
ICU data				
Hospitalization days before ICU entrance, days	1.00 [0.00;3.00]	1.00 [0.00;3.00]	0.730	853
Symptoms to hospital admission, days	7.00 [5.00;10.0]	7.00 [5.00;10.0]	0.667	854
Symptoms to ICU admission, days	9.00 [7.00;11.0]	9.00 [7.00;12.0]	0.478	860
Alive 28 post-ICU discharge, yes	610 (99.5%)	233 (99.1%)	0.621	848
APACHE-II score	11.0 [8.00;14.0]	12.0 [9.00;15.0]	0.040	580
SOFA score	5.00 [4.00;7.00]	5.00 [4.00;7.00]	0.637	628
Arterial blood gas at ICU admission				
pH	7.41 [7.34;7.46]	7.40 [7.34;7.45]	0.331	804
Partial pressure of oxygen, mmHg	79.0 [64.0;103]	79.0 [60.5;100]	0.444	778
Partial pressure of carbon dioxide, mmHg	39.0 [34.0;47.8]	39.0 [34.0;46.0]	0.894	782
Bicarbonate, mmol/L		24.5 [22.0;27.0]	0.497	768
Oxygen saturation, %		95.0 [92.0;97.6]	0.074	809
PaO ₂ to FiO ₂ ratio		119 [83.0;177]	0.502	768
Respiratory rate, rpm		25.0 [21.0;31.0]	0.352	807

Continued on severe page

Baseline sociodemographic and clinical characteristics (at hospital and ICU admission) according DLCO impairment at follow-up visit (*Continuation*)

	DLCO ≥ 60 (n = 624)	DLCO < 60 (n = 237)	p-value	n
	Median [p25;p75] or n (%)	Median [p25;p75] or n (%)		
Pharmacological treatment				
Corticosteroids	517 (83.1%)	197 (83.1%)	0.999	859
Type			0.033	683
Dexametasone	199 (40.0%)	74 (39.8%)		
Metilprednisolone	214 (43.1%)	68 (36.6%)		
Both	65 (13.1%)	40 (21.5%)		
Others	19 (3.82%)	4 (2.15%)		
Dose				
Dexametasone	6.00 [6.00;12.0]	6.00 [6.00;14.2]	0.821	355
Metilprednisolone	15.0 [11.2;46.9]	18.8 [15.0;46.9]	0.116	372
Others	3.75 [3.00;7.50]	7.50 [3.75;7.50]	0.211	73
Anticoagulant	611 (98.1%)	234 (98.7%)	0.771	860
Dose				
Prophylactic dose (< 1 mg/kg/día)	504 (83.2%)	196 (86.0%)	0.382	834
Treatment dose (> 1 mg/kg/día)	238 (39.3%)	89 (39.0%)	0.999	834
Antibiotics				
Hydroxychloroquine	354 (56.7%)	116 (48.9%)	0.049	861
Remdesivir	59 (9.46%)	32 (13.5%)	0.109	861
Tocilizumab	272 (43.6%)	94 (39.7%)	0.335	861
Convalescent plasm	23 (3.70%)	9 (3.80%)	0.999	859
Laboratory data ICU admission				
Hemoglobin, g/dL	13.2 [12.0;14.4]	13.0 [11.9;14.3]	0.407	840
White blood count, × 10 ⁹ /L	8.90 [6.66;11.9]	8.79 [6.59;12.2]	0.820	850
Lymphocyte count, × 10 ⁹ /L	0.70 [0.50;0.95]	0.70 [0.43;0.92]	0.811	845
Neutrophil count, × 10 ⁹ /L	7.70 [5.40;10.5]	7.53 [5.35;10.8]	0.559	845
Monocyte count, × 10 ⁹ /L	0.37 [0.21;0.50]	0.40 [0.22;0.54]	0.242	838
Eosinophil count, × 10 ⁹ /L	0.00 [0.00;0.01]	0.00 [0.00;0.01]	0.559	837
Basophil count, × 10 ⁹ /L	0.00 [0.00;0.02]	0.00 [0.00;0.02]	0.452	838
Hematocrit, %	39.2 [36.3;42.7]	39.0 [36.0;42.7]	0.554	842
Platelet count, × 10 ⁹ /L	234 [189;299]	233 [174;298]	0.541	850
Prothrombin, seconds	13.3 [12.4;14.6]	13.2 [12.2;14.3]	0.178	655
International Normalized Ratio	1.16 [1.09;1.27]	1.13 [1.07;1.24]	0.135	774
D-dimer, mg/L	851 [453;1813]	889 [462;1938]	0.711	735
D-dimer, log	2.93 [2.66;3.26]	2.95 [2.67;3.29]	0.711	735
C-Reactive Protein, mg/dL	155 [87.8;252]	152 [70.0;246]	0.321	816
Glucose, mg/dL	137 [109;181]	134 [112;191]	0.767	838
Bilirubin, mg/dL	0.60 [0.41;0.82]	0.62 [0.48;0.81]	0.647	719
Aspartate transaminase, U/L	49.0 [34.0;74.0]	48.0 [34.0;71.0]	0.513	672
Alanine aminotransferase, U/L	43.0 [27.0;68.0]	40.5 [26.0;60.2]	0.125	810
Urea nitrogen, mg/dL	41.0 [29.2;53.8]	46.0 [31.1;61.0]	0.004	768
Blood urea nitrogen, mg/dL	19.1 [13.6;25.0]	21.4 [14.5;28.6]	0.005	767
Lactate, mmol/L	1.40 [1.00;1.90]	1.35 [1.10;1.80]	0.804	602
Creatinine, mg/dL	0.83 [0.67;1.02]	0.82 [0.66;1.04]	0.966	851
Creatine Kinase, U/L	110 [57.8;211]	79.0 [47.8;141]	0.007	454
Procalcitonin, ng/mL	0.21 [0.11;0.54]	0.19 [0.11;0.44]	0.381	588
Lactate dehydrogenase, U/L	503 [378;706]	480 [380;655]	0.266	681
Sodium, mmol/L	138 [135;140]	137 [135;140]	0.471	846
Potassium, mmol/L	3.99 [3.60;4.32]	4.00 [3.60;4.40]	0.583	838
Albumin, g/dL	3.10 [2.80;3.50]	3.10 [2.84;3.40]	0.738	429
Troponin T, ng/L	0.01 [0.01;0.02]	0.01 [0.01;0.02]	0.147	129
Troponin I, ng/L	0.01 [0.01;0.02]	0.01 [0.01;0.02]	0.867	325
Ferritin, ng/mL	1,418 [758;2,050]	1,280 [764;2,036]	0.761	447
Ferritin, log	3.15 [2.88;3.31]	3.11 [2.88;3.31]	0.761	447
IL6, pg/mL	100 [40.3;240]	114 [61.8;302]	0.084	353
IL6, log	1.97 [1.60;2.33]	2.03 [1.71;2.33]	0.263	330
NT-proBNP, pg/mL	272 [117;534]	357 [148;927]	0.159	155

COPD, chronic obstructive pulmonary disease; HIV, human immunodeficiency viruses; NIMV, non-invasive mechanic ventilation; IMV, invasive mechanic ventilation; ECMO, extracorporeal membrane oxygenation; ARDS, acute respiratory distress syndrome.

Conclusions: In this large cohort of intubated COVID-19 patients, we identified several factors related to IMV associated to an impaired DLCO after hospital discharge. The first clinical scoring tool for the identification patients at high risk of pulmonary sequelae after intubation due to COVID-19 has been developed (<https://trrm.shinyapps.io/CIBERESUCIscore/>).

Funding: ISCIII, UNESPA, CIBERES, FEDER, ESF.

33. ROLE OF CD39 IN COVID-19 SEVERITY: DYSREGULATION OF PURINERGIC SIGNALING AND THROMBOINFLAMMATION

Elena Díaz-García^{1,2}, Sara García-Tovar³, Enrique Alfaro³, Ester Zamarrón³, Alberto Magas³, Raul Galera³, Juan José Ruiz-Hernández⁴, Jordi Solé-Violán⁴, Carlos Rodríguez-Gallego⁴, Ana Van-Den-Rym⁵, Rebeca Pérez de Diego⁵, Kapil Nanwani-Nanwani⁶, Eduardo López-Collazo⁷, Francisco García-Río^{3,8}, Carolina Cubillos-Zapata³

¹Centro de Investigación en Red-CIBERES, Madrid, Spain. ²Grupo de Enfermedades Respiratorias, Servicio de Neumología, Hospital Universitario de La Paz, IdiPAZ, Madrid, Spain. ³Grupo de Enfermedades Respiratorias, Servicio de Neumología, Hospital Universitario de La Paz, IdiPAZ, Madrid, Spain. ⁴Hospital Universitario Dr. Negrín de Gran Canaria, Gran Canaria, Spain. ⁵Grupo de investigación en inmunodeficiencias-IdiPAZ, Madrid, Spain. ⁶Departamento de Medicina Intensiva Hospital Universitario de La Paz, IdiPAZ, Madrid, Spain. ⁷Grupo de inmunidad innata-IdiPAZ, Madrid, Spain. ⁸Facultad de Medicina Universidad Autónoma de Madrid, MADRID, Spain.

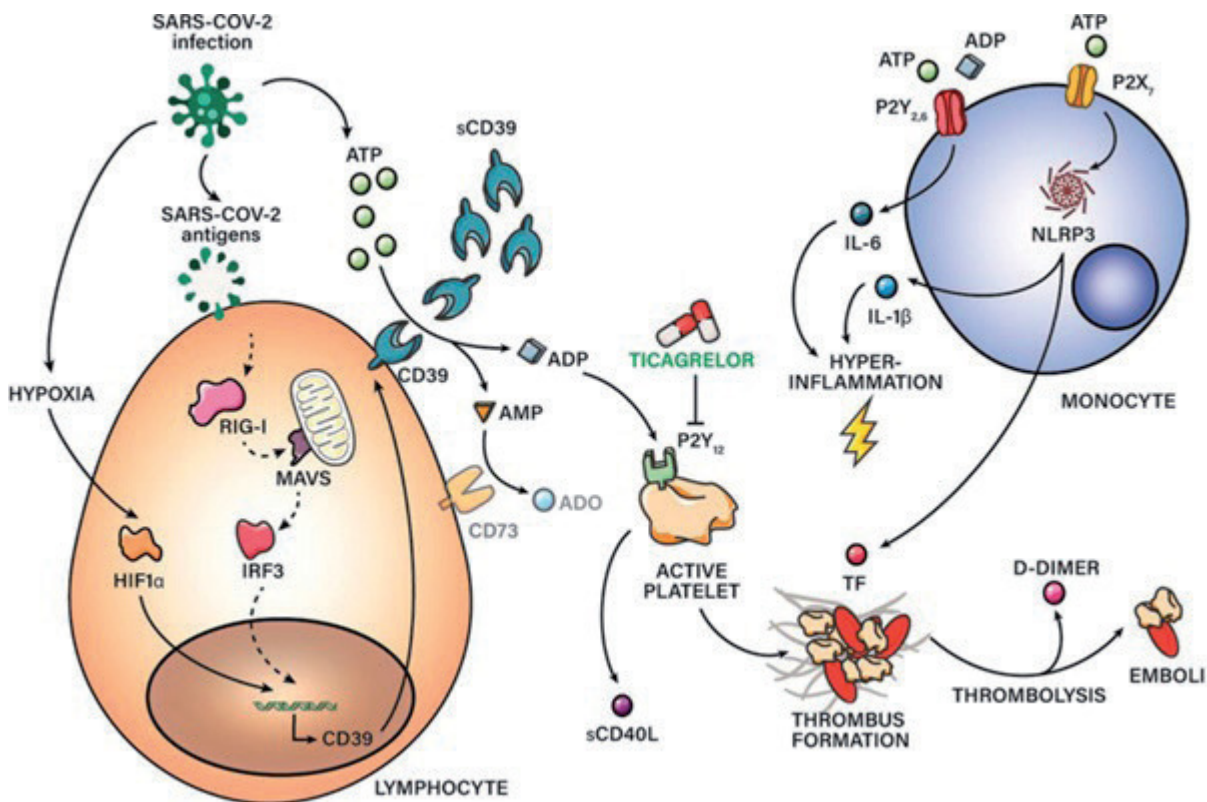
Introduction: Ectonucleoside triphosphate diphosphohydrolase 1 (NTPDase-1 or CD39) is an enzyme capable of hydrolyzing ATP into

ADP and subsequently to AMP. It is expressed in the surface of several cells, including platelets, leukocytes and endothelial cells. CD39 has emerged as an important molecule that contributes to maintain inflammatory and coagulatory homeostasis. Various studies have hypothesized the possible role of CD39 in COVID-19 pathophysiology since no confirmatory data shed light in this regard.

Objectives: We aimed to quantify CD39 expression on COVID-19 patients exploring its association with severity clinical parameters and ICU admission, while unraveling the role of purinergic signaling on thromboinflammation in COVID-19 patients.

Methods: We selected a prospective cohort of patients hospitalized due to severe COVID-19 pneumonia (n = 75), a historical cohort of Influenza A pneumonia patients (n = 18) and sex/age-matched healthy controls (n = 30). Flow cytometry, qPCR and ELISA techniques were performed over patients and donors' plasma and peripheral blood mononuclear cells (PBMCs).

Results: CD39 was overexpressed in COVID-19 patients' plasma and immune cell subsets, and it was related to hypoxemia. Plasma soluble form of CD39 (sCD39) was related to length of hospital stay and independently associated with intensive care unit admission (adjusted odds ratio 1.04, 95%CI 1.0-1.08, p = 0.038), with a net reclassification index of 0.229 (0.118-0.287; p = 0.036). COVID-19 patients showed extracellular accumulation of adenosine nucleotides (ATP and ADP), resulting in systemic inflammation and pro-coagulant state, as a consequence of purinergic pathway dysregulation. Moreover adenosine (ADO) which exerts anti-inflammatory effects was reduced in COVID-19 patients' plasma. Interestingly, we found that COVID-19 plasma caused platelet activation, which was successfully blocked by the P2Y12 receptor inhibitor, ticagrelor (Figure).



CD39 in COVID-19 severity: schematic representation of pro-thrombotic and proinflammatory pathways related with purinergic signaling. sCD39 is upregulated along COVID-19 severity. Hypoxia and antiviral immune response might be involved in CD39 upregulation. Impaired purinergic signaling in COVID-19, characterized by high levels of eATP and eADP in combination with low levels of anti-inflammatory ADO. eATP contribute to hyperinflammation and TF release secondary to NLRP3 activation. eADP overproduction is linked to platelet activation through P2Y12R. Blockade of P2Y12R through drugs as ticagrelor is suggesting as a promising therapy for severe COVID-19 patients.

Conclusions: The study reveals CD39 upregulation in severe COVID-19 patients. The determination of CD39 soluble form in plasma suggests a certain discriminative capacity on the short-to-medium-term prognosis of these patients, so far, its usefulness as a potential biomarker could be evaluated. Moreover, our study indicates that CD39 overexpression in COVID-19 patients could be indicating purinergic signaling dysregulation, which might be at the basis of COVID-19 thromboinflammation disorder.

Funding: This work was supported by the following fundings: Fondo de Investigación Sanitario (FIS)-Fondos FEDER, Spain: P119/01612 (FG-R) and COV20/00207, CP18/00028 and P119-01363 (CC-Z).

42. TISSUE-SPECIFIC GENE EXPRESSION OF IMMUNE-RELATED GENES IN DIFFERENT COVID-19 SEVERITIES

Alberto Gómez-Carballa^{1,2,3}, Irene Rivero-Calle^{4,5,6}, Jacobo Pardo-Seco^{7,8,9}, José Gómez-Rial¹, Gemma Barbeito-Castiñeiras⁴, Carmen Rodríguez-Tenreiro^{7,14}, Xabier Bello^{1,15}, Sara Pischedda^{4,16,17}, María José Currás-Tuala^{2,7,9}, Sandra Viz-Lasheras^{18,19,20}, Federico Martínón-Torres^{16,21,22}, Antonio Salas^{23,24}

¹Genetics, Santiago de Compostela, Spain. ²Unidade de Xenética, Santiago de Compostela, Spain. ³Centro de Investigación Biomédica n Red de Enfermedades Respiratorias (CIBER-ES), Madrid, Spain. ⁴Vaccines and Infections Research Group (GENVIP), Santiago de Compostela, Spain. ⁵Instituto de Ciencias Forenses (INCIFOR), Madrid, Spain. ⁶Translational Pediatrics and Infectious Diseases, Santiago de Compostela, Spain. ⁷Instituto de Investigación Sanitaria de Santiago de Compostela, Santiago de Compostela, Spain. ⁸Facultade de Medicina, Santiago de Compostela, Spain. ⁹Department of Pediatrics, Madrid, Spain. ¹⁰Universidade de Santiago de Compostela, Spain. ¹¹Hospital Clínico Universitario de Santiago de Compostela, Spain. ¹²and GenPoB Research Group. ¹³Centro de Investigación Biomédica en Red de Enfermedades Respiratorias (CIBER-ES), Spain. ¹⁴Instituto de Investigaciones Sanitarias, Madrid, Spain. ¹⁵Hospital Clínico Universitario de Santiago (SERGAS), Santiago de Compostela, Spain. ¹⁶Centro de Investigación Biomédica en Red de Enfermedades Respiratorias (CIBER-ES), Santiago de Compostela, Spain. ¹⁷Translational Pediatrics and Infectious Diseases, Madrid, Spain. ¹⁸Laboratorio de Inmunología. Servicio de Análisis Clínicos. Hospital Clínico Universitario (SERGAS), Santiago de Compostela, Spain. ¹⁹Instituto de Ciencias Forenses (INCIFOR), Santiago de Compostela, Spain. ²⁰Hospital Clínico

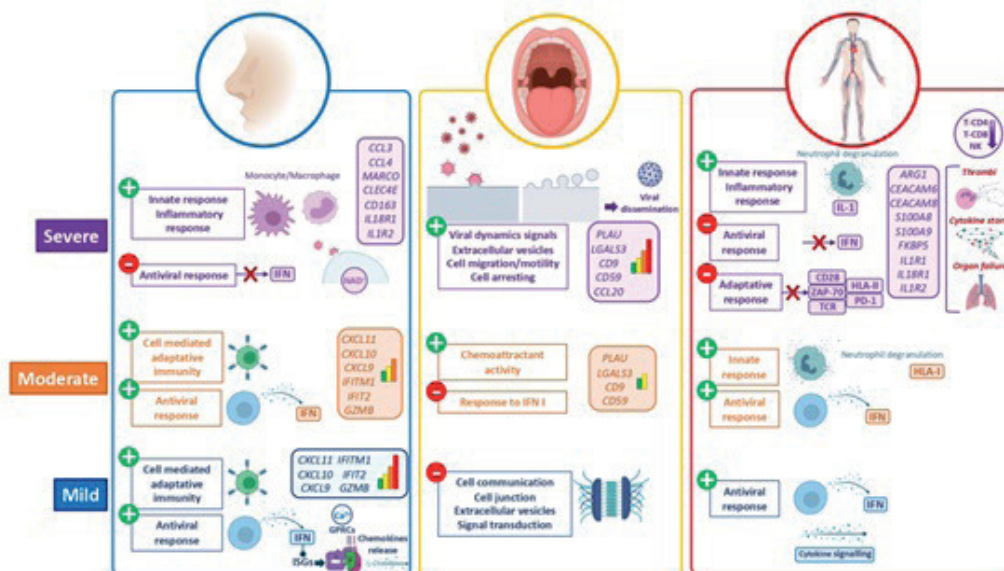
Universitario de Santiago de Compostela, Madrid, Spain. ²¹Clinical Microbiology Unit, Santiago de Compostela, Spain. ²²Facultade de Medicina, Madrid, Spain. ²³Complejo Hospitalario Universitario de Santiago Santiago de Compostela, Santiago de Compostela, Spain. ²⁴Universidade de Santiago de Compostela, Madrid, Spain.

Introduction: Coronavirus Disease-19 (COVID-19) symptoms range from mild to severe illness. The cause for this differential response to infection remains unknown. Unravelling the immune mechanisms acting at different levels of the colonization process might be key to understand these differences.

Objectives: Our study aims at understanding the differential immune response that leads to different disease COVID-19 severities, and find specific severity-related biomarkers or pathways that help to improve patient management and prognostic prediction.

Methods: We carried out a multi-tissue gene expression study of immune-related genes in blood, nasal, and saliva samples, collected on asymptomatic, mild, and severe COVID-19 patients as well as healthy controls (n = 156) through the nCounter technology (Nanostring). We used both an individual gene approach through a differential expression analysis (DESeq2) and a co-expression network approach (WGCNA) followed by a pathway analysis to reveal tissue specific genes and biological routes involved in different severities.

Results: Our results point to a set of genes and pathways that are tissue-specific and correlated to severity, many of these are involved in the innate immune system and cytokine/chemokine signalling pathways. Nasal epithelium showed a robust activation of the antiviral immune machinery in mild cases, characterized by IFN pathway involvement, thus triggering the IFN induced genes and downstream cascades (Th1, NK and T-cytotoxic response) and successfully controlling the infection at local level. Instead, severe cases showed these IFN antiviral response switched off; they develop an innate response represented by an over-expression of genes related to monocyte-macrophage recruitment in nasal epithelium. We did not find signals of immune viral response in buccal mucosa in mild patients, which probably indicates a successful local control of the infection and, therefore, prevention of viral dissemination and systemic colonization. On the contrary, buccal mucosa in moderate and, to a greater extent, severe cases, provided evident signals of viral activity, cell arresting and viral dissemination to the lower respiratory tract, ultimately generating an exacerbated innate and impaired adaptative systemic immune responses in blood (Figure).



Schematic representation of the main findings in gene expression and pathway analysis of COVID-19 severity in nasal, oral and blood tissue.

Conclusions: Local immune response could be key to determine the course of the systemic response and thus COVID-19 severity. Overall, our study highlights the key role of the nasal epithelium in COVID-19 severity, and the importance of the buccal cavity in body infection dissemination. Our findings provide a framework to investigate severity host gene biomarkers and pathways that might be relevant to diagnosis, prognosis, and therapy.

Funding: Agencia Gallega de Innovación (GAIN): GEN-COVID (IN845D 2020/23).

43. THE ROLE OF HOST EPIGENOME IN RESPIRATORY MORBIDITY AFTER RSV INFECTION

Sara Pischedda^{1,2,3}, Irene Rivero-Calle^{3,4}, Alberto Gómez-Carballa^{1,2,3}, Federico Martín-Torres^{3,4,5}, Antonio Salas^{1,3,6}

¹Instituto de Investigación Sanitaria de Santiago de Compostela, Santiago De Compostela, Spain. ²Translational Pediatrics and Infectious Diseases, Department of Pediatrics, Hospital Clínico Universitario de Santiago de Compostela, Santiago de Compostela, Spain. ³Centro de Investigación Biomédica en Red de Enfermedades Respiratorias (CIBER-ES), Madrid, Spain. ⁴Translational Pediatrics and Infectious Diseases, Department of Pediatrics, Hospital Clínico Universitario de Santiago de Compostela, Santiago De Compostela, Spain.

⁵Instituto e Investigación Sanitaria de Santiago de Compostela, Santiago De Compostela, Spain. ⁶Instituto de Ciencias Forenses, Facultade de Medicina, Universidade de Santiago de Compostela, Santiago de Compostela, Spain.

Introduction: Respiratory syncytial virus (RSV) is a common pathogen that infects virtually all children by two years of age and is the leading global cause of hospitalization of infants. RSV infection in infants has been associated with the subsequent development of recurrent wheezing and asthma, although the mechanisms involved are still unknown. Epigenetic regulation behaves as a dynamic interface between genome and environment and in viral infection, this regulation in host defense cells is directly related to disease development

Objectives: The present study aims to assess whether there are differences in the methylation pattern among children who develop recurrent wheezing, children with subsequent asthma, and children experiencing complete recovery after RSV infection.

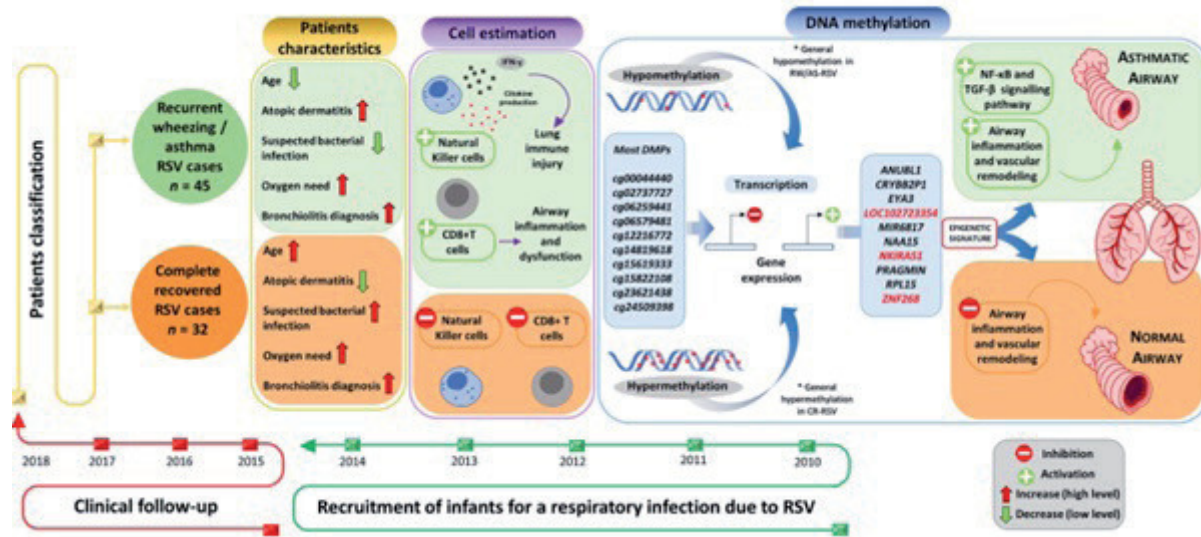
Methods: This is a prospective, observational study of infants admitted for a respiratory infection due to RSV, to the clinical University Hospital of Santiago de Compostela. Patients were selected according to their clinical course and were classified into: recurrent wheezing/asthma RSV cases (RW/AS-RSV, n = 45); and complete recovered RSV cases (CR-RSV, n = 32) (Table). The DNA genome-wide methylation pattern was analysed in whole blood samples, collected during the acute phase of the infection, using the Illumina Infinium Methylation EPIC BeadChip (850K CpG sites). Differences in methylation were determined through a linear regression model adjusted for age, gender and cell composition.

Results: Patients who developed respiratory sequelae showed a statistically significantly higher proportion of NK and CD8T cells (inferred through a deconvolution approach) than those with complete recovery. 5,097 significant differentially methylated positions (DMPs) were identified when comparing RW-RSV and AS-RSV together against CR-RSV. Methylation profiles affect several genes involved in airway inflammation processes. The most significant DMPs were found to be hypomethylated in cases and therefore generally leading to overexpression of affected genes. Logistic regression analysis resulted in a diagnostic epigenetic signature of 3-DMPs (involving genes ZNF2698, LOC102723354 and RPL15/

NKIRAS1) that allows to efficiently differentiate sequelae cases from CR-RSV patients. Genes set analysis revealed a significant enrichment for pathways involved in different cell cycle processes and in the transforming growth factor-beta (TGF- β) signaling pathway (Figure).

Clinical characteristics of patients left for downstream analysis, classified as recurrent wheezing and asthma RSV (RW/AS-RSV) and complete recovery RSV cases (CR-RSV)

	CR-RSV (n = 28)	RW/AS-RSV (n = 40)	P-value
Demographic variables			
Sex Male	17 (60.07%)	28 (70.0%)	0.447
Age in months (mean [SD])*	7.14 [5.32]	5.85 [3.62]	< 0.001
Ethnicity			0.184
Western Europe	24 (85.7%)	36 (90.0%)	-
Southern Europe	2 (7.1%)	1 (2.5%)	-
Southern America	1 (3.6%)	0	-
Roma	0	3 (7.5%)	-
Other	1 (3.6%)	0	-
RSV infection	28 (100.0%)	40 (100.0%)	1
Past medical history prior to RSV-A			
Premature	4 (14.3%)	4 (10.0%)	0.717
Atopic Dermatitis*	2 (7.1%)	13 (32.5%)	0.017
Alimentary allergies	1 (3.6%)	5 (12.5%)	0.399
Stational allergies	0	2 (5.0%)	0.508
Asthma	0	0	1
Admissions prior to RSV	10 (35.7%)	12 (27.0%)	0.399
Annual bronchitis prior the RSV-A*	3 (10.7%)	21 (52.5%)	0.005
Family history			
Asthma	4 (14.3%)	14 (35.0%)	0.052
Respiratory problems	5 (17.9%)	15 (37.5%)	0.053
Clinical characteristics of the RSV-H			
Respiratory distress			0.147
Mild	8 (28.6%)	4 (10.0%)	
Moderate	16 (57.1%)	29 (72.5%)	
Severe	4 (14.3%)	7 (17.5%)	
Oxygen requirement	23 (82.1%)	25 (62.5%)	0.107
Respiratory support			0.128
Non-invasive	3 (10.7%)	8 (20%)	
Mechanical	2 (7.1%)	0	
Diagnosis			0.093
Bronchiolitis	25 (89.3%)	31 (77.5%)	
Bronchospasm	0	1 (2.5%)	
Pneumonia	2 (7.1%)	2 (5.0%)	
Other	1 (3.6%)	6 (15.0%)	
Bacterial superinfection suspected*	20 (71.4%)	12 (30.0%)	<0.001
Follow-up 3 years			
Hospital admission	5 (17.9%)	11 (27.5%)	0.962
Additional episodes of bronchiolitis*	7 (25%)	37 (92.5%)	<0.001



Conclusions: Epigenetic mechanisms might play a fundamental role in the long-term sequelae after RSV infection, contributing to explain the different phenotypes observed.

Funding: This study received support from Instituto de Salud Carlos III (ISCIII), Agencia Gallega de Innovación (GAIN) and consorcio Centro de Investigación Biomédica en Red de Enfermedades Respiratorias (CIBERES).

15. PERIPHERAL ENDOTHELIAL DYSFUNCTION AND ARTERIAL STIFFNESS IN PULMONARY ARTERIAL HYPERTENSION: ASSOCIATION WITH SEVERITY AND CHANGES AFTER TREATMENT

Agustín Roberto García, Isabel Blanco, Yolanda Torralba-García, Clara Martín-Ontiyuelo, Víctor Ivo Peinado, Ana Ramírez-Gallardo, Joan Albert Barberà

Hospital Clínic, Barcelona, Spain.

Introduction: Peripheral arterial dysfunction is considered a biomarker of cardiovascular disease and might be valuable in pulmonary arterial hypertension (PAH), but the relationship is not well established.

Objectives: This study is aimed to correlate peripheral endothelial dysfunction (PED) and arterial stiffness (PAS) with PAH severity and their changes after specific treatment.

Methods: For the cross-sectional study we analyzed 95 PAH patients, including idiopathic (IPAH, n = 39), associated with systemic sclerosis (SSc-PAH, n = 40), and associated with HIV (HIV-PAH, n = 16), and we compared them with 41 healthy subjects and patients with systemic sclerosis (SSc, n = 16) and HIV infection (n = 12) without pulmonary hypertension (PH). PH was ruled out by echocardiography and confirmed by right heart catheterization. PED was evaluated by flow mediated dilatation (FMD) on the brachial artery. PAS was assessed by measuring both pulse wave velocity (PWV) and augmentation index normalized at heart rate of 75 beats per minute (AI75), using applanation tonometry. Fifty-one PAH patients were treatment-naïve (incidents) and 44 prevalent patients. In the 51 incident patients, measurements were repeated after 3 months of specific treatment.

Results: All PAH subgroups had lower FMD and higher both PWV and AI75 compared with healthy subjects, suggesting PED and

higher PAS (Table). Additionally, HIV patients also showed PED regardless PH, while PAS was more associated with baseline SSc. PAS was normal in HIV and trended to increase in IPAH. However, PWV resulted significantly higher in IPAH naïve patients ($9,97 \pm 3.38$ m/s, $p = 0.009$). The magnitude of PAS correlates with exercise limitation and PH severity. PWV correlated with mPAP ($r = -0.3$, $p = 0.012$) and BNP level ($r = +0.4$, $p = 0.03$), and both PWV and AI75 correlated with: WHO-FC, partial pressure of oxygen (PaO₂) and 6-minute walking test (6MWT). Finally, long-term PAH targeted treatment improved peripheral vascular disease. Although we did not find significant improvement in peripheral performance after three months of treatment, those patients under long-term treatment showed significant changes in all FMD, PWV and AI75. Additionally, patients that improved stiffness after treatment also covered longer distance in the 6MWT (+72 vs. +24 m), had greater decrease in BNP (-160 vs. -110 pg/mL) and higher proportion of patients in WHO-FC I-II (63 vs. 50%).

TABLE 4: Cross-sectional subgroup analysis comparing endothelial function and arterial stiffness

	FMD, %	AI75, %	PWV, m/s
Healthy subject (n=41)	11.0 ± 5,3	19,3 ± 10,9	7,1 ± 1,6
IPAH (n=39)	5,2 ± 3,8 *	24,7 ± 13,4	8,3 ± 1,9
SSc-PAH (n=40)	6,9 ± 4,4 * _{ns}	25,4 ± 13,5 *	9,2 ± 2,4 *
HIV-PAH (n=16)	5,3 ± 2,8 *	23,7 ± 4,2 **	7,3 ± 1,1 **
SSc no PAH (n=16)	8,4 ± 4,7	29,8 ± 7,5 *	7,9 ± 2,4
HIV no PAH (n=12)	5,7 ± 2,6 *	8,3 ± 5,8	6,7 ± 0,9

Data are given as median ± interquartile. FMD: flow mediated dilatation expressed as percentage of change from basal; AI75: augmentation index adjusted to heart rate of 75 bpm; PWV: pulse wave velocity; PAH: pulmonary arterial hypertension; IPAH: idiopathic pulmonary arterial hypertension; SSc: systemic sclerosis; HIV: human immunodeficiency virus. * $p < 0.05$ compared with healthy subjects, ** $p < 0.05$ compared with HIV without PAH and # $p < 0.05$ compared with SSc without PAH.

Conclusions: Peripheral arteries are affected in PAH. In HIV the PED is unrelated and probably precedes PH. Patients with SSc have increased PAS, while PED is mainly related to PAH. The higher PAS is associated with exercise limitation and might be useful to assess PAH severity.

Funding: PI12/00510 Instituto de Salud Carlos III, Societat Catalana de Pneumologia (SOCAP) y Fundaci3n Contra la HP (FCHP)

2. INFLAMMASOME ACTIVATION: A KEYSTONE OF PROINFLAMMATORY RESPONSE IN OBSTRUCTIVE SLEEP APNEA

Elena D3az Garc3a¹, Sara Garc3a-Tovar², Enrique Alfar3², Ana Jaureguizar², Raquel Casitas², Bego3a S3nchez-S3nchez², Ester Zamarr3n², Juan Fern3ndez-Lahera², Eduardo L3pez-Collazo², Carolina Cubillos-Zapata¹, Francisco Garc3a-R3o¹

¹CIBERES, Madrid, Spain. ²FIBHULP, Madrid, Spain.

Introduction: Obstructive sleep apnea (OSA) is associated with several inflammatory comorbidities. In the last decades, the NLRP3 inflammasome has emerged as a master regulator in chronic inflammatory disorders. Thus, we hypothesized that NLRP3 inflammasome activation might play a critical role in OSA pathology.

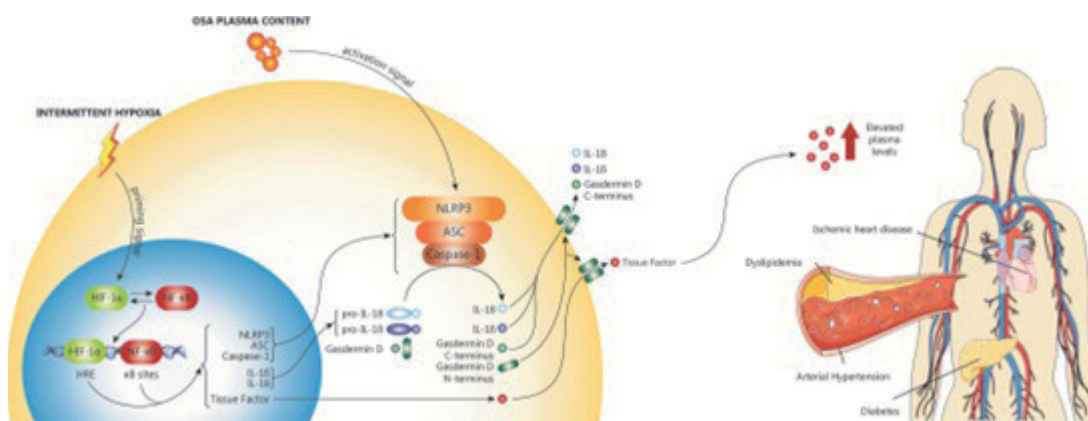
Objectives: We aimed to assess the NLRP3 inflammasome activity in patients with severe OSA and to identify its role in the systemic inflammatory response and subsequent development of comorbidities in these patients.

Methods: We analyzed the NLRP3 inflammasome activity and the expression of key components of the inflammasome cascade, assessing its association with inflammatory comorbidities in patients with severe OSA and control subjects.

Results: Monocytes from patients with severe OSA exhibited higher NLRP3 inflammasome activity than those from control subjects. NLRP3 inflammasome expression was directly related to OSA severity indices and triggered inflammatory cytokines (IL-1 β and IL-18) and tissue factor (TF) release. *In vitro* models confirmed that intermittent hypoxia triggers the NLRP3 inflammasome priming signal (in a hypoxia-inducible factor-1 α (HIF-1 α) dependent manner) while the activation signal is mediated by OSA plasma-soluble factors. Finally, plasma levels of TF were higher in patients with OSA with inflammatory comorbidities than in those without them (Figure).

Adjusted comparison of study variables between the study groups. Values are mean \pm standard error of the mean (SEM). Adjusted comparisons were performed with general linear models using a univariate analysis of variance with the study group as fixed variable and sex, age, BMI and diagnosis of type 2 diabetes as covariates

	Severe OSA patients		Non-apneic control subjects		p
	n	Adjusted mean \pm SEM	n	Adjusted mean \pm SEM	
CD14+ NLRP3+ cells, %	51	48.6 \pm 2.5	24	20.4 \pm 3.8	< 0.001
CD14+ CASP1+ cells, %	44	56.4 \pm 3.6	24	9.0 \pm 5.0	< 0.001
CD14+ ASC+ cells, %	44	41.6 \pm 3.3	24	27.5 \pm 4.5	0.015
HIF-1 mRNA expression, \times 103	40	1.2 \pm 0.3	20	0.2 \pm 0.03	0.001
mTOR mRNA expression, \times 103	40	14.8 \pm 3.0	34	1.4 \pm 0.3	< 0.001
NF κ B mRNA expression, \times 103	16	13.8 \pm 7	16	0.4 \pm 0.2	0.008
NLRP3 mRNA expression, \times 103	68	3.9 \pm 0.7	40	0.3 \pm 0.9	0.002
ASC mRNA expression, \times 103	37	8.1 \pm 1.8	26	1.6 \pm 1.5	0.008
CASP1 mRNA expression, \times 103	38	1.1 \pm 0.2	39	0.3 \pm 0.1	< 0.001
GSDMD mRNA expression, \times 103	40	5.7 \pm 1.1	14	2.5 \pm 2.0	0.075
TF mRNA expression, \times 102	52	7.0 \pm 1.6	19	0.6 \pm 2.7	0.042
IL-18 mRNA expression, \times 103	30	23.1 \pm 4.7	36	2.0 \pm 4.3	0.002
IL-1 β mRNA expression, \times 102	31	9.9 \pm 2.8	38	0.4 \pm 2.5	0.010
TF serum level, pg/ml	95	139.1 \pm 8.0	20	47.6 \pm 17.1	< 0.001
GSDMD serum level, pg/ml	95	4.6 \pm 0.5	20	1.1 \pm 1.1	0.005
IL-18 serum level, pg/ml	64	1147 \pm 194	20	104 \pm 349	0.021
IL-1 β serum level, pg/ml	80	4.1 \pm 0.2	20	2.4 \pm 0.2	< 0.001



Summary of proinflammatory role of NLRP3 (nucleotide-binding oligomerization domain-like receptor 3) activation in patients with obstructive sleep apnea (OSA). In patients with OSA, HIF1 α (hypoxia-inducible factor 1 α) signaling is triggered by intermittent hypoxia and, in combination with NF- κ B (nuclear factor- κ B) induction, promotes the transcription of the main components of the inflammasome. This constitutes the priming step necessary for NLRP3 inflammasome activation. Unidentified plasma soluble factors act as the "activation signal" leading to complete activation of the NLRP3 inflammasome. The activation of NLRP3 drives the formation of a multiprotein complex, which leads to the recruitment and activation of caspase-1 and subsequent processing of the mature forms of IL-1 β and IL-18. Caspase-1 also cleaves GSDMD (Gasdermin D), which then forms cytolytic pores, leading to pyroptosis and IL-1 β , IL-18 and tissue factor (TF) release. NLRP3 activation results in an increase in the levels of IL-1 β , IL-18, and TF in plasma. Lastly, elevated circulating TF might be a potential biomarker to discriminate between patients with severe OSA with comorbidities such as dyslipidemia, diabetes, hypertension, or ischemic heart disease. ASC = adaptor molecule apoptosis-associated speck-like protein; HRE = hypoxia-response element.

Conclusions: Severe OSA increases the activity of the NLRP3 inflammasome by triggering both the priming signal and the activation signal. Additionally, this study suggests the potential role of TF as a molecular biomarker for inflammatory disorders in OSA patients. **Funding:** Supported by grants from Fondo de Investigación Sanitaria (FIS) and European Regional Development Funds (FEDER) (PI13/01512, PI16/00201, and PI19/01612 to F.G.-R. and CP18/00028 and PI19-01363 to C.C.-Z.).

8. CHARACTERIZATION OF THE MECHANISMS OF CARDIOVASCULAR RECURRENCE INDUCED BY OSA IN PATIENTS WITH ACUTE CORONARY SYNDROME: A POST-HOC ANALYSIS FROM THE ISAACC STUDY

Andrea Zapater^{1,2}, Esther Gracia-Lavedán^{2,3}, Gerard Torres^{2,3}, Mario Henríquez^{3,4}, Olga Mínguez³, Lydia Pascual³, Anunciación Cortijo³, Dolores Martínez³, Iván David Benítez^{2,3}, Ferran Barbé^{2,3}, Manuel Sánchez de la Torre^{1,2}

¹Group of Precision Medicine in Chronic Diseases, Respiratory Department, University Hospital Arnau de Vilanova and Santa María; Department of Nursing and Physiotherapy, Faculty of Nursing and Physiotherapy, University of Lleida. IRBLleida, Lleida, Spain. ²Centro de Investigación Biomédica en Red de Enfermedades Respiratorias (CIBERES), Madrid, Spain. ³Translation Research in Respiratory Medicine, Hospital Universitari Arnau de Vilanova-Santa Maria, IRBLleida, Lleida, Spain. ⁴Escuela de Kinesiología, Facultad de Salud Universidad Santo Tomás, Los Angeles, Chile.

Introduction: Obstructive sleep apnea (OSA) has been associated with increased risk of recurrent cardiovascular event (CVE) in a specific endotype of patients with acute coronary syndrome (ACS). However, the pathophysiological mechanisms underlying OSA associated with the recurrence of CVE have not been elucidated.

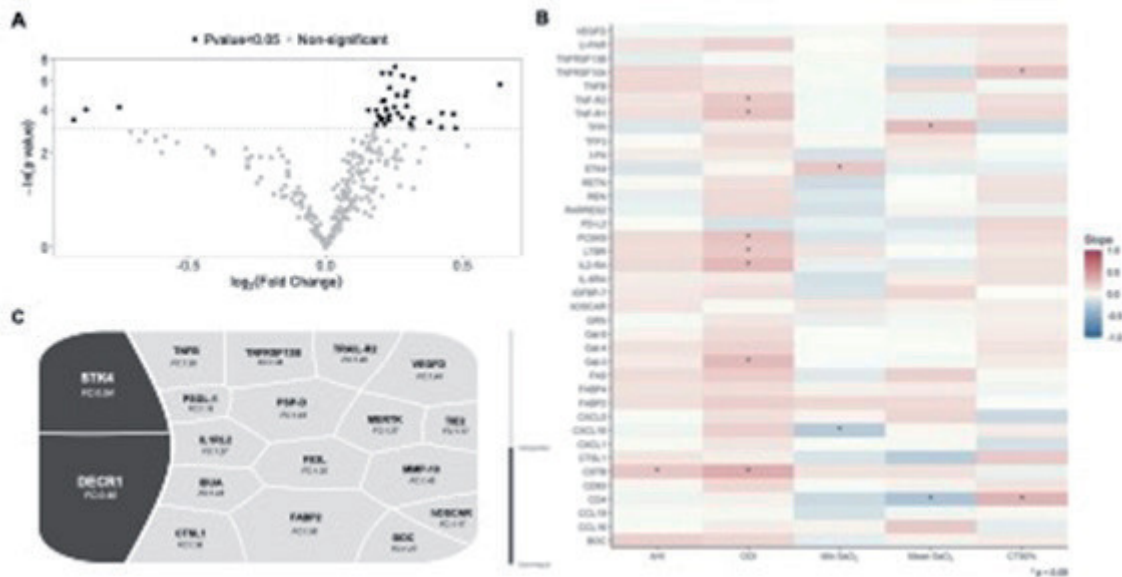
Objectives: We aim to characterize the differential proteomic profile in patients with ACS and recurrent CVE, according to the presence or absence of OSA.

Methods: For the current post-hoc analysis of the ISAACC study (NCT01335087), we included 58 patients admitted for ACS without previous cardiovascular disease. Patients underwent a polygraphy the first 24-72 h to evaluate the presence of OSA. We analyzed 276 cardiovascular and inflammatory related protein biomarkers in fasting plasma samples using Proximity Expression Assay technology (Olink®, Sweden).

Results: We enrolled 58 patients with ACS and recurrent CVE during the follow-up (median age: 58 years, median BMI: 28.6 kg/m² and 77.6% males): 28 patients without OSA and 30 patients with severe OSA. A total of 24 proteins had differential plasma levels between groups (Figure A). Additionally, respiratory polygraphy parameters commonly used for OSA diagnosis (apnea-hypopnea index, desaturation index, medium and minimum SaO₂ and time with SaO₂ < 90%) were associated with 18 of the differentially expressed proteins (Figure B). The expression of each biomarker between groups showed an overexpression of 16 of them in OSA patients (Figure C). These proteins were implicated in biological pathways such as immune system, hematopoiesis and different cell processes (Figure).

Conclusions: In patients with ACS and a recurrent CVE, OSA would be associated with the activation of specific molecular pathways that would promote cardiovascular recurrence. The identified biomarkers were involved in endothelial dysfunction, oxidative stress and systemic inflammation, intermediate mechanisms linking OSA with its cardiovascular consequences.

Funding: Instituto de Salud Carlos III (ISCIII) (PI10/02763, PI10/02745, PI18/00449, PI21/00337), co-funded by the European Union, IRBLleida-Fundació Dr.Pifarré, CERCA Programme/Generalitat de Catalunya, SEPAR, ResMed Ltd. (Australia), Esteve-Teijin (Spain), Oxigen Salud (Spain) ALLER and SES.



Differential protein plasma levels according to OSA condition in ACS patients with recurrent CVE. (A) Volcano plot shows the negative logarithm of the p-value versus the log₂ fold change for each detected protein. Horizontal dashed line indicates a cutoff of 0.05 for p value. Black dots are detected proteins with significant differences in plasma levels between groups. (B) Linear association between identified proteins and respiratory polygraphy parameters adjusted by confounding factors, such as age, sex, BMI and hypertension. Linear model was used to assess the association between identified proteins (outcome) and respiratory polygraphy parameters. All variables were standardized. Slope between identified proteins and respiratory polygraphy parameters are represented through a color scale with red tones related to positive association and blue tones related to negative association. *Significant p-values (p < 0.05). (C) Voronoi treemaps of differentially expressed proteins. The sizes of the polygons reflect the magnitude of the fold change. Upregulated or down-regulated proteins grouped by identical color schemes are shown in the figure, along with the name of each protein. OSA: Obstructive sleep apnea, ACS: Acute coronary syndrome; CVE: cardiovascular event, AHI: Apnea-Hypopnea Index; ODI: Oxygen desaturation index; SaO₂: Oxygen saturation

12. TEMPORAL TRENDS OF ADULT INVASIVE PNEUMOCOCCAL DISEASE CAUSED BY SEROTYPE 3 FROM 1994 TO 2019

Sara Calvo-Silveria¹, Aida González-Díaz¹, Fe Tubau¹, Jordi Càmarà¹, Anna Carrera-Salinas¹, Inmaculada Grau¹, Roman Pallares¹, Sara Marti¹, Jose Yuste², Carmen Ardanuy¹

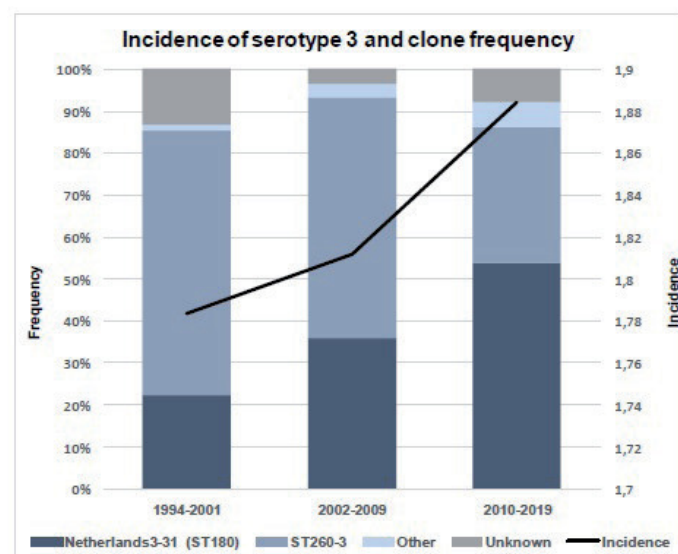
¹Hospital de Bellvitge, Hospitalet de Llobregat, Spain. ²Instituto de Salud Carlos III, Madrid, Spain.

Introduction: *Streptococcus pneumoniae* has more than 95 serotypes, but only a few of them cause disease. Pneumococcal conjugated vaccines (PCV) were introduced to prevent pneumococcal disease. In Spain, PCV7 was introduced in 2001 and replaced by PCV13 in 2010.

Objectives: The aim was to analyse the epidemiology and antibiotic resistance of serotype 3 causing invasive pneumococcal disease (IPD) in adults (≥ 18 years).

Methods: All cases of adult IPD (1994-2019) from patients admitted to Hospital Universitari de Bellvitge were prospectively collected. IPD was defined as the isolation of *S. pneumoniae* in a sterile site. Three study periods were defined: pre-PCV (1994-2001), PCV7 (2002-2009) and PCV13 (2010-2019). The incidence was calculated as number of episodes per 100,000 inhabitants. Genotype was determined by pulsed-field gel electrophoresis and antimicrobial susceptibility was studied following EUCAST criteria.

Results: A total of 267 episodes of serotype 3 from IPD were detected during the study period, being pneumonia the main cause of infection (65.9%). The overall incidence initially increased from 15.11 to 19.13 (pre-PCV to PCV7) and then decreased to 17.14 in PCV13 period. The incidence due to serotype 3 (Figure) remained stable along time (1.78 to 1.81 and 1.88). Over the study period, frequency of serotype 3 in young adults (18-64 years) increased from 6.6 to 7.5 to 9.7% and in older adults (> 65 years) decreased from 17.8 to 11.7 to 11.9%. Two major clonal complexes, which accounted for 85% of episodes, were identified: ST2603 and Netherlands3-31 (ST180). A progressive shift in their frequency was observed being ST260 more prevalent in pre-PCV and PCV7 periods (63.2 and 57.3%, respectively) and Netherlands3-31 in PCV13 period (53.9%) (Figure). Serotype 3 isolates presented low antibiotic resistance rates; 26 isolates (9.7%) were resistant to co-trimoxazole, 15 (5.6%) to tetracyclines and 7 (2.6%) to erythromycin and clindamycin.



Frequency of clonal complex and incidence of serotype 3.

Conclusions: Serotype 3, included in PCV13, is still one of the most frequent cause of IPD. The clonal shift observed over the last years may have contributed to its persistence as an important cause of disease. Further studies will be needed to analyse the impact on upcoming vaccines in this serotype.

Funding: This study was funded by Instituto de Salud Carlos III (ISCIII) through the Projects "FIS21/01000" and "FIS18/00339", Centro de Investigación Biomédica en Red (CIBER) de Enfermedades Respiratorias (CIBERes) "CB06/06/0037" and MISP Programm (MSD).

50. ONE-HEALTH GENOMIC ANALYSIS OF A SELF-LIMITED TUBERCULOSIS FAMILIAR MICROEPIDEMIC REVEALS A LONG-TERM UNNOTICED ZOOZONOSIS INVOLVING MYCOBACTERIUM CAPRAE

Laura Pérez-Lago¹, Miguel Martínez-Lirola¹, Marta Herranz², Cristina Rodríguez-Grande¹, José Antonio Garrido³, Ana Belén Esteban García³, Francisca Escabia Machuca³, María Teresa Cabezas Fernández², Sergio Buenestado-Serrano¹, José María Viudez Martínez⁵, Eva Domínguez Inarra⁶, Patricia Muñoz⁷, Darío García de Viedma⁸

¹Instituto de investigación Sanitaria Gregorio Marañón, Madrid, Spain. ²Complejo Hospitalario Torrecárdenas, Almería, Spain. ³Universidad de Almería, Almería, Spain. ⁴Unidad de Prevención, Promoción y Vigilancia de la Salud del Área Sanitaria Norte de Almería, Almería, Spain. ⁵Oficina Comarcal Agraria de Huerca-Overa, Junta de Andalucía, Almería, Spain. ⁶Laboratorio de producción y Sanidad Animal, Junta de Andalucía, Córdoba, Spain. ⁷Instituto de Investigación Sanitaria Gregorio Marañón; CIBERES; Universidad Complutense de Madrid, Madrid, Spain. ⁸Instituto de Investigación Sanitaria Gregorio Marañón; CIBERES, Madrid, Spain.

Introduction: Molecular epidemiology identifies transmission chains that can be refined with the application of WGS. We present a MIRU-VNTR cluster interpreted as a familiar microepidemic (year 2020; cases A and B). WGS revealed that the isolates corresponded to *M. caprae*, which is not routinely identified to the species level in many laboratories. Cases A and B were interviewed and they acknowledged to own a goat farm. These findings led us to retrospectively look for other *M. caprae* cases, which could have been unnoticed, as well as the study of the extent of infection on the farm.

Objectives: Better understanding of a MIRU-VNTR cluster without clear epidemiological explanation, and complete genomic data about its transmission environment.

Methods: WGS was performed on MIRU-VNTR cluster for complete understanding of the transmission chain. Because of the zoonosis finding, we followed a one-health approach to integrate in our investigation the animal analysis. Twelve additional cases along the 2003-19 period shared MIRU-VNTR similar patterns were included in the WGS analysis.

Results: The SNP-distances and genomic relationships between the isolates reinterpreted this familiar cluster, ruling out Case A-Case B direct transmission. A high rate of infection was found in the farm studied (124/350 positive animals); *M. caprae* was isolated from 11/24 necropsies cultured. All additional cases with MIRU-VNTR similar patterns were confirmed by WGS as *M. caprae*. The integrated WGS analysis of all the human and animal isolates identified a cluster that included the year 2020 Case A and B isolates and those of 9 goats and a high diversity of *M. caprae* strains for the remaining human isolates.

Conclusions: The integration of population-based MIRU-VNTR analysis together with a more refined genomic analysis, under a one-health strategy, has revealed an extense endemic zoonotic problem involving *M. caprae*, unnoticed for more than 10 years.

Funding: Junta de Andalucía (AP-0062-2021-C2-F2), ISCIII (PI21/01823, PI19/00331, FI20/00129) and FEDER fund "A way of making Europe".

20. POTENTIAL BIOMARKERS FOR THE DIAGNOSIS OF PATIENTS WITH LUNG FIBROSIS

Silvia Sánchez-Díez^{1,2}, Xavier Muñoz^{1,2,3}, David Espejo¹,
Íñigo Ojanguren^{1,2}, Christian Romero-Mesones¹, María Jesús Cruz^{1,2}

¹Pulmonology Service, Department of Medicine, Vall d'Hebron University Hospital, Autonomous University of Barcelona, Barcelona, Spain. ²CIBER of Respiratory Diseases (CIBERES), Madrid, Spain. ³Department of Cell Biology, Physiology and Immunology, Autonomous University of Barcelona, Barcelona, Spain.

Introduction: Hypersensitivity pneumonitis (HP) is an interstitial lung disease (ILD) characterized by a bronchoalveolar inflammation that occurs in genetically predisposed individuals after the inhalation of organic or inorganic compounds. Up to 40% of the cases progress to pulmonary fibrosis, suffering a significant loss of lung function with the development of respiratory failure that leads to death if a lung transplant is not carried out.

Objectives: The aim of this study was to determine the possible involvement of the innate and adaptive immune responses in the development of pulmonary fibrosis in tissue samples of patients with advanced fibrotic HP who underwent lung transplant.

Methods: Cross-sectional study conducted in 18 patients diagnosed with fibrotic HP and 10 patients diagnosed with idiopathic pulmonary fibrosis (IPF) who underwent lung transplantation. Healthy donors (n = 8) were included as control groups. Lung samples were obtained from Vall d'Hebron and Ciberes Biobanks. Cytokines with a Th1, Th2 and Th17 profile were determined in the tissue homogenate supernatant and MUC16 biomarker of fibrosis progression was also analyzed in paraffin-embedded lung samples.

Results: Both patients with fibrotic HP and IPF had higher levels of IL-7, IL-13, IL-17 and IL-23 compared to healthy donors, while the levels of IL-1 β and GM-CSF were increased in patients with fibrotic HP but not in patients with IPF. Fifty per cent of patients with fibrotic HP had a more pronounced Th2 profile with higher levels of IL-5 and IL-6. This group of patients also had increased levels of IL-1 β , IL-8, G-CSF and MCP-1, and lower levels of GM-CSF and IL-23 compared to HP patients with a no Th2 profile. HP patients with an Th2 profile also had higher levels of TNF α while the others exhibited increased levels of IL-2 compared to healthy controls. Maximum expression of MUC16 was observed in patients with IPF.

Conclusions: Both patients with fibrotic HP and IPF have increased levels of Th17-related cytokines. The immunological response in HP patients with a more Th2 profile seems to indicate a more pronounced activation of the adaptive immune response with high production of cytokines involved in the recruitment of granulocytes.

Funding: Study funded by ISCIII (PI18/00345), FEDER and FUCAP.

23. MUSCLE PHENOTYPIC FEATURES IN THE VASTUS LATERALIS OF PATIENTS WITH BRONCHIECTASIS

Adriana Núñez Robainas^{1,2,3}, Mariela Nieves Alvarado Miranda^{1,2,3},
María Pérez Peiró^{1,2,3}, Esther Barreiro^{1,2,3}

¹Pulmonology Department, Muscle Wasting and Cachexia in Chronic Respiratory Diseases and Lung Cancer Research Group, IMIM-Hospital del Mar, Parc de Salut Mar, Barcelona, Spain. ²Department of Medicine and Life Sciences (MELIS), Universitat Pompeu Fabra (UPF), Barcelona Biomedical Research Park (PRBB), Barcelona, Spain. ³Group CB06/06/0043 of Centro de Investigación en Red de Enfermedades Respiratorias (CIBERES), Instituto de Salud Carlos III (ISCIII), Barcelona, Spain.

Introduction: In patients with chronic respiratory inflammatory diseases, muscle weakness is a common feature. So far, the systemic

manifestations of bronchiectasis characterized by recurrent exacerbations and inflammation have not been studied yet.

Objectives: In the vastus lateralis (VL) samples of control subjects and bronchiectasis patients, we sought to study muscle phenotypic features including muscle regeneration and muscle morphometry.

Methods: Ten healthy subjects and twenty stable bronchiectasis patients were recruited. Nutritional and functional parameters were evaluated. In the VL of the participants, muscle fiber type, morphometry, and structural abnormalities were assessed; apoptotic-nuclei were quantified using the TUNEL assay and counting techniques (conventional immunohistochemistry) and total numbers of satellite cells were measured through identification of markers Pax7 and Myf5 (conventional immunofluorescence with specific antibodies and fluorochromes).

Results: Compared to control subjects, bronchiectasis patients presented a significant reduction in nutritional and muscle functional parameters such as body weight, body mass index (BMI), fat free mass index (FFMI) and overall muscle strength (hands and quadriceps). Blood nutritional parameters such as urea, A1 antitrypsin, ceruloplasmin and Erythrocyte Sedimentation Rate (ESR) significantly increased compared to control subjects, while albumin and pre-albumin levels decreased. Hybrid fiber proportion was greater in bronchiectasis patients compared to controls, while type II and hybrid fibers presented smaller cross-sectional areas (CSA). Muscle abnormalities, internal nuclei and TUNEL-positive nuclei proportions were significantly increased in bronchiectasis patients. In addition, quiescent cell counts (Pax7+/Myf5-) and total satellite cell counts were substantially reduced in patients with bronchiectasis compared to control subjects, while committed cells (Pax7+/Myf5+) were significantly increased.

Conclusions: In the lower limb muscles of bronchiectasis patients, there are significant alterations in the muscle phenotype and metabolic features being the most relevant the presence of greater proportions of hybrid fibers and smaller cross-sectional areas of type II and hybrid fibers. Moreover, bronchiectasis patients presented muscle structural abnormalities mainly by a rise in the proportions of internal nuclei and apoptotic nuclei (TUNEL). Finally, patients presented an increase of activated satellite cells, which suggest the trigger of muscle regeneration. These findings will help elucidate the impact of bronchiectasis in the muscle physiology and function.

Funding: FIS 21/00215 (FEDER, ISC-III), Intensificación INT19, CIBERES (ISC-III), SEPAR Ayudas a la Investigación 2020.

32. CHARACTERIZATION OF THE SKELETAL MUSCLE-SPECIFIC AND INDUCIBLE BMAL1 KNOCKOUT MOUSE (IMS-BMAL1-/-) AS A MODEL FOR THE STUDY OF SARCOPENIA AND EVALUATION OF EXERCISE AND/OR MELATONIN TREATMENTS

José Fernández-Martínez^{1,2,3}, Yolanda Ramírez-Casas^{1,2,3},
Paula Aranda-Martínez^{1,2,3}, Germaine Escames^{1,2,3},
Darío Acuña-Castroviejo^{1,2,3}

¹Departamento de Fisiología, Facultad de Medicina, Centro de Investigación Biomédica, Universidad de Granada, Granada, Spain.

²Centro de Investigación Biomédica en Red de Fragilidad y Envejecimiento Saludable (CIBERfes), Madrid, Spain. ³Instituto de Investigación Biosanitaria de Granada (Ibs.Granada), Granada, Spain.

Introduction: Sarcopenia is an age-related disease characterized by a reduction in muscle mass, strength and function and, therefore, a deterioration in skeletal muscle health and frailty. It is a serious problem due to the aging of the population and because there is currently no treatment. Although the cause of sarcopenia is still unknown, increasing evidence suggests that disruption of the biological clock can yield mechanisms that ultimately lead to sarcopenia.

Objectives: To analyze whether disruption of Bmal1 clock gene, which has anti-inflammatory properties and enhances mitochondrial function, and its expression decreases with age, may be related to sarcopenia. For this purpose, we developed a skeletal muscle-specific and inducible Bmal1 knockout murine model (iMS-Bmal1^{-/-}) to study the relationship between chronodisruption, inflammation, mitochondrial dysfunction and muscle loss in aging, and then assess the efficacy of a therapeutic intervention with exercise and/or melatonin.

Methods: To generate the conditional knockout, tamoxifen-induced Cre-LoxP recombination was activated by intraperitoneal injections of tamoxifen (2 mg/day) for five consecutive days when the mice reached 12 weeks. Phenotyping, histological, and transmission electron microscopy (TEM) analysis were performed when mice reached 15 weeks of age, except for the circadian rhythm assessment of locomotor activity, that started at week 14.

Results: Phenotypic studies performed (SMART, Treadmill, ClockLab, gastrocnemius muscle weight/body weight ratio, and frailty index (FI)) revealed a significant drop in muscle function, a phase advance in the circadian rhythm of locomotor activity, and a significant increased frailty in iMS-Bmal1^{-/-} mice compared with controls. Histological and TEM analysis showed alterations in the structure and ultrastructure of gastrocnemius muscle in iMS-Bmal1^{-/-} mice compared to controls, especially evident at the mitochondrial level. Exercise and/or melatonin ameliorated the damage caused by loss of Bmal1 in mutant mice.

Conclusions: iMS-Bmal1^{-/-} mice let us to identify Bmal1 deficiency as the responsible for the onset of chronodisruption, which may underlie the muscular deficit of the gastrocnemius muscle, i.e. sarcopenia. Moreover, the results support the exercise and melatonin as therapeutic tools to counteract sarcopenia.

Funding: Financial support was provided by grants PI2019/01372 and CIBERfes (ISCIII). Y.R.-C. has a PFIS (ISCIII) fellowship, and J. F.-M. a FPU fellowship (Ministerio de Educación).

27. RUCAPARIB ATTENUATES TUMOR BURDEN THROUGH OXIDATIVE STRESS IN AN EXPERIMENTAL MODEL OF LUNG ADENOCARCINOMA

Maria Pérez Peiró^{1,2}, Paula Valentí Serra¹, Blanca León González¹, Coral Ampurdanés³, Xavier Duran⁴, José Yélamos³, Esther Barreiro^{1,2}

¹Pulmonology Department-Muscle Wasting and Cachexia in Chronic Respiratory Diseases and Lung Cancer Research Group, IMIM-Hospital del Mar, Parc de Salut Mar, Department of Medicine and Life Sciences (MELIS), Universitat Pompeu Fabra (UPF), Barcelona Biomedical Research Park (PRBB), Barcelona, Spain. ²Centro de Investigación en Red de Enfermedades Respiratorias (CIBERES), Instituto de Salud Carlos III (ISCIII), Grupo CB06/06/0043, Barcelona, Spain. ³Cancer Research Program, Hospital del Mar Medical Research Institute (IMIM)-Hospital del Mar, Barcelona, Spain. ⁴Scientific, Statistics, and Technical Department, Hospital del Mar-IMIM, Parc de Salut Mar, Barcelona, Spain.

Introduction: Non-small cell lung cancer (NSCLC) is one of the leading causes of cancer death worldwide. Poly (ADPribose) polymerases (PARP)-1 and PARP-2 play a critical role in DNA repair in healthy cells. However, cancer cells also use this repair mechanism to survive. PARP inhibitors are currently approved for the pharmacological treatment of several cancer types, such as ovarian and breast cancer. We hypothesized that that treatment with rucaparib, a PARP inhibitor, may reduce tumor burden via several biological mechanisms in a mice model.

Objectives: In the subcutaneous tumors (LP07 lung adenocarcinoma cells) of mice treated with this PARP inhibitor the objectives are the

following: 1) to assess PARP activity and protein PARP expression; 2) to evaluate DNA damage; 3) to examine cell proliferation; 4) to analyze pro-oxidant and antioxidant markers.

Methods: Experimental groups: 1) tumor-bearing mice treated with rucaparib (150 mg/kg body weight/24h for 20-day, N = 10) and 2) control tumor-bearing mice not receiving the pharmacological treatment (0.5% methylcellulose/24h for 20-day, N = 10). In the tumors of all study mice, PARP activity (polymers of poly (ADP-ribose) (PAR), immunohistochemistry and immunoblotting), PARP expression (PARP-1 and PARP-2, immunoblotting), cell proliferation (ki-67, immunohistochemistry), DNA damage (γ -H2AX, immunohistochemistry), pro-oxidant and antioxidant markers (protein carbonylation, MDA-protein adducts, protein nitration, SOD-1, SOD-2 and catalase, immunoblotting) were quantified. Body weight and tumor area were also evaluated in all the study mice.

Results: Rucaparib-treated mice showed a reduction in tumor area while body weight improved in comparison to non-treated mice. PARP activity was significantly reduced in rucaparib-treated mice, while no differences were observed in either PARP-1 or PARP-2 protein levels between the study groups. In the tumors of rodents treated with rucaparib compared to non-treated mice, levels of DNA damage significantly increased, whereas the cell proliferation marker ki-67 decreased. Levels of total protein carbonylation as measured by reactive carbonyls and MDA-protein adducts and those of SOD-2 protein significantly increased in rucaparib-treated tumor-bearing mice compared to the untreated animals.

Conclusions: In this experimental mouse model of lung adenocarcinoma, the pharmacological PARP activity inhibitor rucaparib decreased tumor size in the treated animals, probably through decreased cell proliferation as a result of increased DNA damage. These results highlight the contribution of PARP inhibitors to the reduction of tumor burden in lung adenocarcinoma. However, further studies in clinical settings of patients with lung tumors are still needed to explore its potential implications.

Funding: FI-19/00001, FIS 18/00075 (FEDER), CIBERES, and SEPAR 2018.

44. STUDY OF THE EFFICACY OF INTRAVENOUS BCG IN A METASTATIC LUNG ADENOCARCINOMA MOUSE MODEL

Claudia Guerrero, Eduardo Moreo, Santiago Uranga, Ana Belen Gomez, Carlos Martín, Nacho Aguiló

Universidad de Zaragoza, Zaragoza, Spain.

Introduction: Bacillus Calmette-Guérin (BCG) is a live attenuated mycobacterium vaccine and it is at present the only tuberculosis vaccine used in humans. Since more than four decades ago, intravesical BCG represents a gold standard therapy for high-risk non-muscular invasive bladder cancer. Recently, systemic delivery of BCG has recently been reported to drive profound changes in bone marrow (BM) myelopoiesis providing a more efficient capacity of response against a subsequent tuberculosis infection. However, i.v. BCG has never been studied in the context of orthotopic lung tumors.

Objectives: The aim of this project is to study the antitumoral response of intravenous (i.v.) BCG in a metastatic lung adenocarcinoma mouse model.

Methods: In order to develop a metastatic lung adenocarcinoma mouse model, lungs with adenocarcinoma of mice-bearing KrasG12V mutation were collected and a lung cell suspension was generated. This suspension was inoculated subcutaneously to C57BL/6 mice. The tumor developed, called KC8.1, was collected and expanded in order to create a cell line (KC8.1 cell line). To study the efficacy of i.v. BCG, mice were vaccinated intravenously with 106 CFU of BCG after or pri-

or to KC8.1 tumor challenge. Flow cytometry was used to study population cells in lungs and spleen. Cell suspension was generated to study cytokine levels by ELISA. A congenic bone marrow transplant model was developed to study the effect of i.v. BCG in the bone marrow.

Results: Mice inoculated with i.v. BCG prior to tumor cells inoculation showed higher survival compared to non-treated mice. However, i.v. BCG delivery after tumor challenge did not provide any therapeutic advantage, suggesting that tumor might be influencing i.v. BCG efficacy. A congenic BM transplant mouse model suggested the ability of i.v. BCG to re-educate haematopoietic progenitors to overcome tumor influence. Moreover, prior administration of i.v. BCG avoided myeloid-derived suppressor cells (MDSCs) accumulation in lungs of tumor-bearing mice, in contrast to i.v. BCG after tumor challenge leading to an immunosuppressive ambience. Finally, therapeutic combination of i.v. BCG with gemcitabine, which reduce MDSCs at low doses, further increased mouse survival compared to gemcitabine in monotherapy.

Conclusions: As a result, combination of i.v. BCG with chemotherapy could represent an attractive therapeutic approach for advanced lung cancer.

Funding: AECC, Asociación Española Contra el Cáncer. Diputación General de Aragón.

49. EXPERIMENTAL LUNG CANCER MODEL AND SMOKING EFFECTS

Laura Sánchez Carretero¹, Sandra Pérez Rial^{1,2}, Oderay Mabel Cedeño Díaz³, Jordi Llop Roig^{4,2}, Jesús Ruiz Cabello^{5,2}, Luis M. Seijo Maceiras^{6,2}, Germán Peces-Barba^{1,2}

¹IIS-Fundación Jiménez Díaz (Experimental Pulmonology Laboratory), Madrid, Spain. ²Consortio Centro de Investigación Biomédica en Red, M.P. de Enfermedades Respiratorias (CIBERES), Madrid, Spain.

³IIS-Fundación Jiménez Díaz (Pathological Anatomy Department), Madrid, Spain. ⁴CICbiomaGUNE (Radiochemistry and Nuclear Imaging Lab), Gipuzkoa, Spain. ⁵CICbiomaGUNE (Molecular and Function Lab) at Biomarkers in Cardiovascular and Pulmonary Disease Lab), Gipuzkoa, Spain. ⁶Clínica Universidad de Navarra (CUN), Madrid, Spain.

Introduction: This is a preliminary communication of the ECCO project (PI20-01416) that studies the interaction between lung cancer (LC), COPD and SAHS. They are very common respiratory diseases, whose confluence is not rare and whose main trigger is tobacco.

Objectives: The main objective of this preliminary communication is to observe the effect of tobacco on tumor development and progression in lung cancer.

Methods: We used an experimental model of lung cancer, chronically exposed to tobacco smoke (3R4F). For this, female mice of the susceptible strain A/J01aHsd are initially administered with a carcinogen, 4-methylnitrosamine-1-(3-pyridyl)-1-butanone (NNK), injected intraperitoneally at a rate of 100 mg/kg. Half of them were also exposed to tobacco smoke for 6 months. The evolution of the body weight gain of the mice is recorded once a month. Before necropsies, pulmonary ventilation is studied by PET/CT using a radioactive gas (SF6); and the lung function of the mice is also analyzed. The lungs are then removed, from which a histological image and a gene expression study are obtained by qPCR of 84 genes related to oncogenesis, angiogenesis and hypoxia.

Results: In the context of lung cancer, tobacco produces a decrease in body weight gain from the fifth month of exposure; it produces a functional irregularity in the ventilation of smokers' lungs, with hypoventilated areas; decreases the maximum inspiratory and ex-

piratory volume to 25mbar. Regarding tumor histology, there is an increase in the number of tumors and the total tumor area, as well as an increase in the area of pure papillary tumors. The gene expression of lung tissue is modified by the effect of tobacco, decreasing the expression levels of several genes related to tumor proliferation (Angptl6, Cdknia (p21), Cdkn2b (p15), Igf1, Igfbp4, NFkbia...).

Conclusions: In the experimental model of lung cancer, we have found that tobacco alters tumor histology, both in extension and in the type of tumor induced by the carcinogen. Furthermore, in the context of cancer, tobacco seems to decrease the expression of certain genes related to tumor proliferation. These conclusions are open until the results of the control group without lung cancer are available.

Funding: This work has been funded by Instituto de Salud Carlos III (Proyect PI20-01416).

53. ENGINEERED BACTERIA AS A NEW THERAPY FOR P. AERUGINOSA BIOFILMS IN CRITICALLY ILL PATIENTS

Laia Fernández-Barat¹, Alba Soler-Comas², Anna Motos¹, Rocco Mazzolini², Alicia Broto Hernández², Irene Rodríguez Arce², Nil Vázquez¹, Roberto Cabrera¹, Luis Serrano², Maria Lluch-Senar², Antoni Torres³

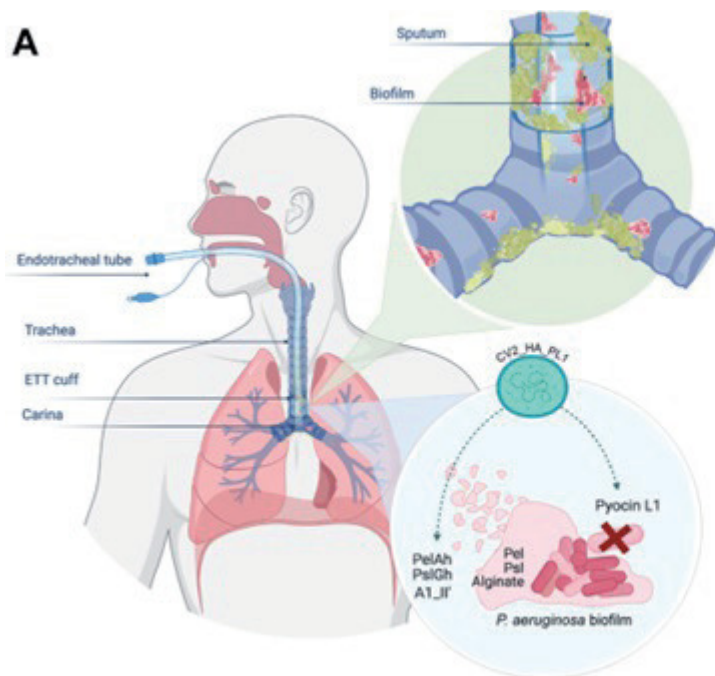
¹Ciberes-IDIBAPS, University of Barcelona, Barcelona, Spain. ²Centre for Genomic Regulation, Barcelona, Spain. ³Pneumology Department, Hospital Clinic of Barcelona, Barcelona, Spain.

Introduction: Biofilms are the predominant living strategy in most bacterial species and cause between 60-80% of human infections, accounting for a major burden to healthcare systems. In patients under invasive mechanical ventilation, biofilms develop in the endotracheal tube (ETT) lumen and become an important focus of pathogens causing ventilator-associated pneumonia (VAP) or its relapse. As functionally heterogeneous multi-cellular communities, biofilms grow encased in a self-produced matrix, attached to abiotic and biotic surfaces, and are tolerant to antimicrobials and host immune defenses. In this framework, a genetically modified *M. pneumoniae* strain has been deprived of its non-essential native genes and has become one of the first bacterial lung "chassis" (CV2_HA_PL1) which locally delivers specific biofilm dispersal (alginate lyase and hydrolases) and killing (pyocin-L1) agents against *P. aeruginosa* (Figure 1A).

Objectives: To test the *ex vivo* efficacy of this new "chassis" against *P. aeruginosa* ETT-biofilms obtained from mechanically ventilated patients with *P. aeruginosa* VAP.

Methods: Human ETTs (Collection R190311-203; HCB/2019/0262) were selected from patients ventilated during 11 [6.00-16.50] days, and with confirmed presence of *P. aeruginosa* in ETT (2.57 [2.20-4.81] log₁₀ CFU/ml) at extubation. Fourteen ETT hemisections were exposed for 24 h to control (Hayflick medium alone without treatment, n = 3), CV2_HA_PL1 (#casi10⁸ Log CFU/mL, n = 4), Ceftolozane-Tazobactam (5 µg/ml, n = 4), CV2_HA_P1 + Ceftolozane-Tazobactam (n = 3). The CV2_HA_P1 inoculum contained 7.32 [8.26-9.20] Log CFU/mL. *P. aeruginosa* counts (Log CFU/mL) after treatment were reported, as well as antimicrobial susceptibility and phylogenetic analysis by multi-locus sequence typing (using eBURST algorithm) were carried out.

Results: *P. aeruginosa* counts showed significant differences between groups. ETT-biofilm treated with antibiotics reduced the *P. aeruginosa* load. This reduction was higher with the CV2_HA_P1 alone and even more clinically significant when combined with antibiotics (Figure 1B). The *P. aeruginosa* isolates were resistant to Meropenem (100%), Imipenem (100%), Aztreonam (100%), Amika-



B

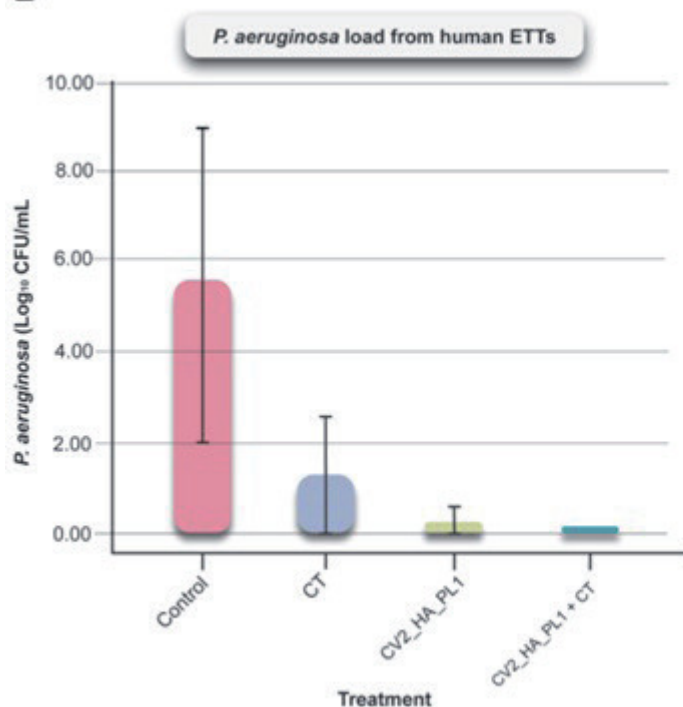


Figure 1

A) ETT biofilm formation in mechanically ventilated patients in risk of developing ventilator-associated pneumonia (VAP). The following close-up shows an overview of how the chassis works. *Mycoplasma pneumoniae* has been engineered by plugging in an optimized genetic platform that encodes for different proteins with activity against the main components of *P. aeruginosa* biofilms. PelAh and PslGh glycoside hydrolases and A1_IF alginate lyase have been selected to destroy Pel and Psl exopolysaccharides and alginate, respectively, thus allowing the dispersion of biofilms^{1, 2, 3}. Moreover, pyocin L1 has been chosen as an antimicrobial agent since it is a lectin-type bacteriocin that specifically targets *P. aeruginosa*.

B) Effect of treatment on ETT biofilm from ICU patients. This graphic depicts the *P. aeruginosa* median [IQR] load (Log₁₀ CFU/mL) in each treatment group: control (Hayflick medium alone without treatment, n=3), CV2_HA_PL1, Ceftolozane-Tazobactam, CV2_HA_P1 + Ceftolozane-Tazobactam. Significant differences between groups were found ($p = 0.049$, Kruskal-Wallis test). The median and the interquartile range [IQR] load (log₁₀ CFU ml⁻¹) of each treatment group were: 1. control: 7.51 [4.44–7.51]; 2. Ceftolozane-Tazobactam: 0.77 [0.00–2.52]; 3. CV2_HA_P1: 0.00 [0.00–0.52]; 4. CV2_HA_P1 + Ceftolozane-Tazobactam: 0.00 [0.00–0.00]. The p-values for pairwise comparisons between groups (Wilcoxon signed-rank test) were: 2 to 1: $p=0.150$; 3 to 1: $p=0.026$; 4 to 1: $p=0.034$; 3 to 2: $p=0.321$; 4 to 2: $p=0.186$; 4 to 3: $p=0.386$. Levels of significance for pairwise comparisons was $p=0.008$.

References

¹ Pestrak, M. J. et al. Treatment with the *Pseudomonas aeruginosa* Glycoside Hydrolase PslG Combats Wound Infection by Improving Antibiotic Efficacy and Host Innate Immune Activity. *Antimicrob. Agents Chemother.* 63, (2019).

² Blanco-Cabra, N. et al. Characterization of different alginate lyases for dissolving *Pseudomonas aeruginosa* biofilms. *Sci. Rep.* 10, 9390 (2020).

³ Ghequire, M. G. K. et al. O serotype-independent susceptibility of *Pseudomonas aeruginosa* to lectin-like pyocins. *Microbiology Open* 3, 875–884 (2014).

cin (66%), and Ciprofloxacin (33%) but were susceptible to Colistin, Piperacillin-Tazobactam, Tobramycin and Ceftazidime. The ST109 and ST259 strains were allocated to the clonal complex 253 and 2044 previously described in ICU patients and bronchiectasis, respectively.

Conclusions: CV2_HA_P1 has a broad spectrum effect against biofilm formed by different multidrug-resistant *P. aeruginosa* clinical strains, which are otherwise difficult to eliminate using conventional antimicrobial treatment.

Funding: La Caixa Health 2018 (code: HR18-00058) to L. Serrano and A. Torres.

21. EFFECTS OF HYPERCAPNIA ON ALVEOLAR EPITHELIAL CELLS AND MACROPHAGES INFECTED WITH PNEUMONIA-CAUSING BACTERIA

Elena Campaña-Duel¹, Luís Morales-Quinteros^{1,2,3}, Adrian Ceccato^{1,4}, Aina Areny-Balagueró^{1,2}, Pamela Conde^{4,5}, Lluís Blanch^{1,2,4,6}, Laia Fernández^{4,5}, Antonio Artigas^{1,2,4,6}, Marta Camprubí-Rimblas^{1,2,4}

¹Parc Taulí Hospital Universitari, Institut d'Investigació i Innovació Parc Taulí (I3PT), Sabadell, Spain. ²Universitat Autònoma de Barcelona, Bellaterra, Spain. ³Intensive Care, Hospital de la Santa Creu i Sant Pau, Barcelona, Spain. ⁴Centro de Investigaciones Biomédicas en Red de

Enfermedades Respiratorias (CIBERES), Madrid, Spain. ⁵IDIBAPS/ Fundació Clínic, Barcelona, Spain. ⁶Critical Care Center, Corporació Sanitària i Universitària Parc Taulí, Sabadell, Spain.

Introduction: *Streptococcus pneumoniae* is the most frequent cause of community-acquired pneumonia, while *Pseudomonas aeruginosa* leads in nosocomial respiratory infections. Patients with advanced lung disease commonly develop hypercapnia. In vitro infection models are crucial to study the relationship between the cells of the alveolus and pathogens, and the role of hypercapnia in this interaction.

Objectives: To evaluate the inflammatory response, cellular junctions and apoptosis of alveolar epithelial cells (HPAEpiC) and macrophage-like THP-1 cells in co-culture as a result of infection with different types of bacteria (*P. aeruginosa* and *S. pneumoniae*) under different CO₂ concentrations.

Methods: Co-cultures of human pulmonary alveolar epithelial cells (HPAEpiC) and macrophage-like THP-1 cells were separately infected with *Pseudomonas aeruginosa* (MOI 1:50) or *Streptococcus pneumoniae* (MOI 1:20) for 1h at 37 °C under normocapnic (5% CO₂) or hypercapnic (15% CO₂) conditions. Bacterial survival post-infection was evaluated. 24h after infection, at 37 °C and 5% or 15% CO₂, cell culture supernatant and intracellular protein were analysed through ELISA technique for inflammatory (IL-1 β), chemoattractant (IL-8, CCL-2) and cell junction (ZO-1) mediators. Apoptosis was also assessed by TUNEL assay.

Results: Infection with *P. aeruginosa* in a culture of HPAEpiC and THP-1 cells under hypercapnia increases inflammation, and decreases phagocyte chemotaxis and THP-1 cell apoptosis compared to normocapnic conditions. In contrast, *S. pneumoniae* infection in a culture of HPAEpiC and THP-1 cells under hypercapnia increases inflammation and decreases phagocyte chemotaxis compared to normocapnic conditions, and impedes bacterial clearance probably through intracellular niche establishment (Figure).

Conclusions: A culture of alveolar epithelial cells and THP-1 macrophage-like cells infected by *P. aeruginosa* and *S. pneumoniae* performs different defensive responses. Hypercapnic condition on bacterial-in-

fection response could play a beneficial role in *P. aeruginosa* infection, but a detrimental role in *S. pneumoniae* infection.

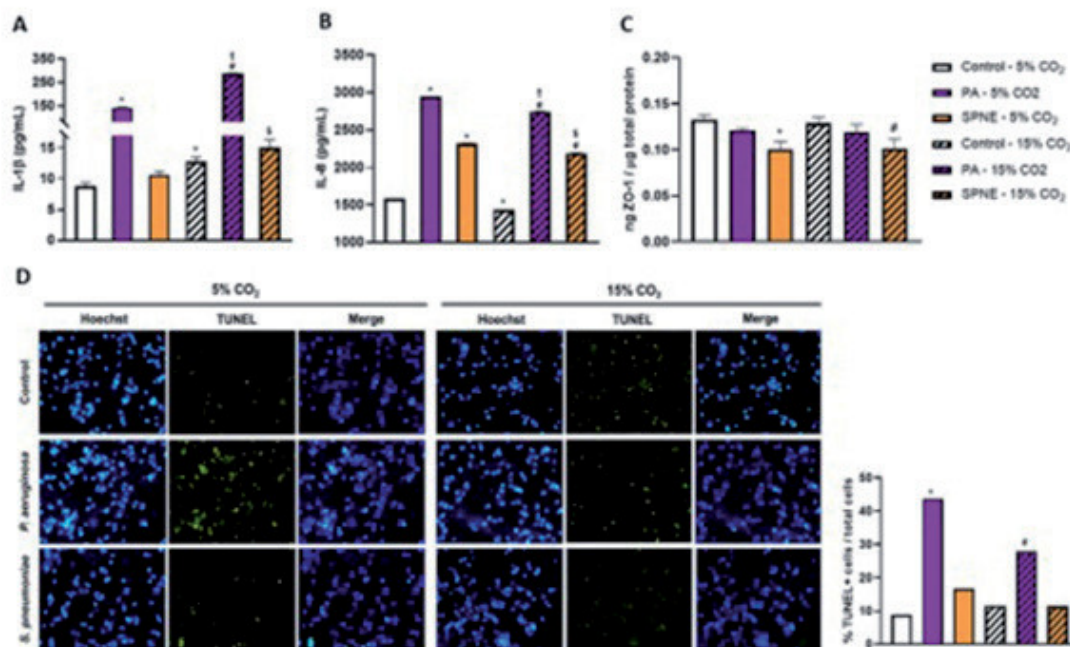
Funding: This project was supported by Sociedad Española de Neumología y Cirugía Torácica (SEPAR); European Society of Intensive Care Medicine (ESICM); Parc Taulí Hospital Universitari, Institut d'Investigació i Innovació Parc Taulí (I3PT) and Centro de Investigación Biomédica en Red de Enfermedades Respiratorias (CIBERes).

47. TRANSCRIPTOMIC SIGNATURES OF LUNG STRETCH

Paula Martín-Vicente^{1,2}, Cecilia López-Martínez^{1,2}, Laura Amado-Rodríguez^{1,2,3}, Inés López-Alonso^{1,2}, Margarita Fernández-Rodríguez^{1,4}, Adrián González-López^{2,5}, Pablo Martínez-Cambor⁶, Andrew J Boyle⁷, Cecilia M O'Kane⁷, Daniel f Mcauley⁷, James N Tsoaporis⁸, Claudia Dos Santos⁸, Guillermo M Albaiceta^{1,2,3,4}

¹Instituto de Investigación Sanitaria del Principado de Asturias (ISPA), Oviedo, Spain. ²Centro de Investigación Biomédica en Red (CIBER)-Enfermedades Respiratorias, Instituto de Salud Carlos III, Madrid, Spain. ³Unidad de Cuidados Intensivos Cardiológicos. Hospital Universitario Central de Asturias, Oviedo, Spain. ⁴Departamento de Biología Funcional, Instituto Universitario de Oncología del Principado de Asturias, Universidad de Oviedo, Oviedo, Spain. ⁵Department of Anesthesiology and Operative Intensive Care Medicine CCM/CVK, Charité-Universitätsmedizin Berlin, corporate member of Freie Universität Berlin, Humboldt Universität zu Berlin, and Berlin Institute of Health, Berlin, Germany. ⁶Department of Biomedical Data Sciences, Geisel School of Medicine, Dartmouth College, Hanover, United States. ⁷Wellcome-Wolfson Institute for Experimental Medicine, School of Medicine Dentistry and Biomedical Science, Queen's University, Belfast, United Kingdom. ⁸Keenan Research Centre for Biomedical Science, St Michael's Hospital, Toronto, Canada.

Introduction: Overstretching of lung parenchyma may lead to tissue injury, especially during mechanical ventilation. To date, there are no specific biomarkers of lung stretch, but transcriptomic signatures of



Inflammation, tight junction and apoptosis analysis 24h post-infection. Protein concentration in cell culture supernatant of proinflammatory mediators (IL-1 β) (A) and chemokines (IL-8) (B) and ZO-1 protein concentration in total intracellular protein (C) 24 h post-infection with *P. aeruginosa* or *S. pneumoniae* of the HPAEpiC and THP-1 cells co-culture. Apoptosis was assessed in THP-1 cell cultures infected with *P. aeruginosa* or *S. pneumoniae* 24 hours post-infection (D). Analysis was done through fluorescence microscopy, TUNEL+ cells were then quantified among total cells. n = 9-12 in protein analysis and n = 2 in TUNEL assay. Data represented as mean \pm SEM. *p = 0.05 vs Control - 5% CO₂. #p = 0.05 vs Control - 15% CO₂. †p = 0.05 vs PA - 5% CO₂. \$p = 0.05 vs SPNE - 5% CO₂. PA: *P. aeruginosa*. SPNE: *S. pneumoniae*. ZO-1: zonula occludens.

micro-RNAs and genes have not been explored. We hypothesized that alveolar-capillary membrane distension and cyclic deformation is associated with the quantifiable presence of specific miRNAs.

Objectives: To identify transcriptomic signatures of micro-RNAs and genes associated with injurious mechanical stretch and validate them in preclinical models.

Methods: In order to identify stretch-specific signatures, data on micro-RNA expression in response to stretch in experimental models were systematically pooled. Signatures were identified as those micro-RNAs or genes with differential expression in samples from stretched cells, and optimized using a greedy algorithm. Transcriptomic scores were calculated as the difference of geometric means in expression of up- and down-regulated features, and compared among different magnitudes of stretch. The accuracy of these scores was validated in animal models of lung injury, *ex vivo* mechanically ventilated human lungs and in bronchoalveolar lavage fluid (BALF) from patients under different ventilatory conditions.

Results: Eight micro-RNAs were differentially expressed in stretched cell cultures ($n = 24$). Amongst the genes regulated by these micro-RNAs, a 180-gene signature was identified in *in vitro* models ($n = 106$) and using data from animal models ($n = 143$) a 4-gene signature (LYPLA1, TXNIP, MX2, F3) was established. The transcriptomic score calculated using only these genes showed significant differences between ventilated and non-ventilated animals and an excellent accuracy for stretch detection. The micro-RNA signatures were validated in human tissue and BALF, and the micro-RNA score was calculated using the abundance of the target micro-RNAs. This score had an area under the ROC curve between 0.89 and 1 respectively to identify lung overdistention.

Conclusions: Lung cell stretch induces the expression of specific micro-RNA and genes. These signatures may be used to obtain an index of lung overstretching that can be measured at the bedside.

Funding: Supported by Centro de Investigación Biomédica en Red (CIBER)-Enfermedades Respiratorias.

29. LPS TREATMENT ENHANCES THE IMMUNOMODULATORY EFFECT OF MESENCHYMAL STROMAL CELLS-DERIVED EXTRACELLULAR VESICLES

Aina Areny-Balaguero^{1,2}, Marta Camprubí-Rimblas^{1,2,3}, Elena Campaña-Duel¹, Daniel Closa⁴, Antonio Artigas^{1,2,3,5}

¹Institut d'Investigació i Innovació Parc Taulí, Sabadell, Spain.

²Universitat Autònoma de Barcelona, Bellaterra, Spain. ³Centro de Investigaciones Biomédicas en Red de Enfermedades Respiratorias, Madrid, Spain. ⁴Institut d'Investigacions Biomèdiques de Barcelona, Sabadell, Spain. ⁵Servei de Medicina Intensiva, Corporació Sanitària i Universitària Parc Taulí, Sabadell, Spain.

Introduction: Sepsis is an aberrant or dysregulated immune response to infection that leads to life-threatening organ dysfunction, affecting principally the lungs and causing, in many cases, an acute respiratory distress syndrome (ARDS). ARDS is associated with a mortality rate of 40% and its biological heterogeneity is one of the main reasons why there is still a lack of a definitive treatment. Extracellular vesicles (EVs) secreted by mesenchymal stromal cells (MSCs) have been widely described for their immunomodulatory and regenerative function of injured tissues, which are essential aspects to treat sepsis and its consequent organ dysfunction.

Objectives: In this study we aimed to determine the effect of the MSCs-derived EVs on immune response in an acute lung injury (ALI) pre-clinical model, and to study how priming MSCs with lipopolysaccharide (LPS) affect their therapeutic potential.

Methods: The ALI model was induced in Sprague-Dawley rats (#casi250 g) by the intratracheal administration of 300 μ l HCl (0.1M) and 2 h later 500 μ l LPS (30 μ g/g body weight). Nine hours (h) after

the injury, animals were administered with 500 μ l of Control EVs or LPS EVs, isolated from MSCs supernatant (cultured with or without LPS). Control animals received saline (0.9%) instead. Animals were sacrificed after 72 h. Pro-inflammatory and chemoattractant mediators were evaluated in lung tissue and bronchoalveolar lavage (BAL) macrophages at mRNA levels. Flow cytometry was used to perform differential and total cell count on BAL. Statistics: One-Way-ANOVA and Newman Keuls *post-hoc* test was used (Statistical significance: $p \leq 0.05$).

Results: Regarding the inflammation in lung tissue, we observed that both control and LPS EVs reduced the expression of inflammatory cytokines (IL-1 β and IL-6) and chemoattractants (CCL2 and CXCL-1), as well as, in the macrophages present in BAL, which in addition, showed an increased expression of M2 phenotype markers, such as Mannose Receptor (MR) and Arginase-1 (Arg-1). However, only animals treated with LPS EVs showed a decrease in cell infiltration in the intralveolar space. In fact, they exhibited a significant reduction of the percentage of neutrophils in BAL.

Conclusions: Priming MSCs with LPS enhances the immunomodulatory effect of their secreted EVs in a pre-clinical model of ALI. Further studies are required to evaluate the effect of LPS EVs on lung tissue injury restoration.

Funding: This project was supported by Ministerio de Economía y Competitividad - Instituto de Salud Carlos III (PI18/00677), Fundación Ramon Areces (CIVP19S8207), I3PT and CIBERES.

45. LUNG EXTRACELLULAR MATRIX HYDROGELS - DERIVED NANOPARTICLES CONTRIBUTE TO EPITHELIAL LUNG REPAIR

Anna Ulldemolins¹, Alicia Jurado², Jorge Otero^{3,4,5}, Ramon Farré^{1,4,6}, Isaac Almendros^{2,4,6}

¹Unitat de Biofísica i Bioenginyeria, Barcelona, Spain. ²Facultat de Medicina i Ciències de la Salut, Barcelona, Spain. ³Universitat de Barcelona, Barcelona, Spain. ⁴CIBER Enfermedades Respiratorias, Madrid, Spain. ⁵IBEC, Barcelona, Spain. ⁶IDIBAPS, Barcelona, Spain.

Introduction: Mesenchymal stem cells (MSCs) cultured in physiometric natural lung-derived hydrogels (L-HG) increased their therapeutic capacity in an *in vitro* model of acute lung injury. Furthermore, MSCs-derived extracellular vesicles (EVs) have demonstrated therapeutic potential to mitigate or even reverse tissue damage in lung diseases. However, recent data has shown that L-HG could release other bioactive extracellular matrix-derived nanoparticles which could also contribute to lung repair.

Objectives: Here, we aim to understand the therapeutic capacity of EVs released from MSCs and/or HGs in an experimental model of lung repair.

Methods: EVs released from MSCs cultured in L-HG and conventional culture were isolated. The particles of the different cell culture conditions were characterized, and their therapeutic capacity was tested by using an alveolar epithelial wound-healing assay.

Results: The EVs released from acellular L-HG were 10-fold greater than those obtained from MSCs in conventional culture revealing that L-HG is an important source of EVs which could interact with alveolar epithelial cells during MSCs driven lung repair. Wound healing assay confirmed that both, MSCs-derived EVs and decellularized extracellular matrix-derived nanoparticles, have a similar therapeutic capacity. However, when wound closure rate was normalized by total protein, the MSCs-derived EVs shows higher therapeutic potential to those released by L-HG.

Conclusions: These results revealed that physiometric L-HG is an important source of therapeutic EVs which must be considered when it is used as substrate for MSCs cell culture and EVs isolation.

Funding: Ministerio de Ciencia e Investigación (PID2019-108958RB-I00/AEI/10.13039/501100011033) and SEPAR.